TABLE 3. LIST OF ADVERSE EVENTS

Type of event	*No. of cases*
Severe adverse event	
Meniscal tear[a]	1
Nonsevere adverse event	
Increase of creatine phosphokinase, increase of C-reactive protein	10
Anemia	9
Pain of hip joint, decrease of albumin, complication of postoperative wound	8
Decrease of total protein, postoperative wound pain	6
Fever	5
Back pain, astriction, increase of glutamate oxaloacetate transaminase	4
Pain around injection, pain of extremity, hyposthesia of lower extremity	3
Decrease of body weight, increase of aspartate aminotransferase, inflammation around continuous epidural anesthesia catheter, cough, red patch around wound, insomnia, muscular pain, nausea, itching sensation, increase of white blood cell, stiffness of muscle, nausea after injection, secretion around the drainage, pharyngeal pain	2
Abdominal pain, itching around wound, rare around bandage, decrease of lactase dehydrogenase, increase of lactase dehydrogenase, increase of potassium, increase of blood pressure, dehydration, contact dermatitis, vertigo, difficulty of urination, headache, hypertension, increase of uric acid, keroid scar, dullness, stiffness around the clavicle, musculoskeletal pain, nasopharyngitis, orthostatic hypotension, fracture of the rib, dental pain, transient vocal cord paresis, increase of body weight, bleeding after injection, dyschezia, itching around eye, electrolyte abnormality, vomiting after surgery, headache after surgery	1

[a]Medial meniscus tear in the contralateral knee joint.

1988 to 1997 in the affiliated hospital. The proportion of nonprogressed case in that series was 26/38 (68%), while the proportion of nonprogressed case in the current series was 7/9 (78%, 95% CI: 40–97%). Although it is clear that the prospective randomized trial using enough number of patients is necessary to draw any conclusion, the result in this study suggested the feasibility of our method. Based on the results in this study, we re-evaluate the risk–benefit value of each step and will modify to improve the value in the next trials.

Whether transplanted cells exert therapeutic effects through direct differentiation to osteogenic cells remain to be investigated. Most initial cell transplantation studies were designed and performed with the aim of engrafting transplanted cells to regenerate the tissue. However, recent studies showed that this was not the case. Only a small proportion of MSCs, locally or systemically administrated, will actually be incorporated into injured tissues, which indicates that the beneficial effects of tissue repair and regeneration are more likely indirect and depend on the paracrine activity of MSCs.[45,46] This should be also considered in our case, although it is difficult to trace the fate of transplanted cells in humans.

As a conclusion, we showed that our procedure was performed safely, but the efficacy was still to be determined. In addition to the increase in the sample number, future modification should be considered to increase the efficacy, such as the combination with suitable degradable artificial components and growth factors. Information from the current clinical trial may lead to the successful result for the advanced stage of ION.

Acknowledgments

The authors are grateful to Drs. Kei-ichiro Kawanabe and Haruhiko Akiyama for their technical advice on ION, Drs. Kazumi Miura, Tatsuya Ito, Akira Shimizu, and Ryota Asada for promoting the clinical study, and Drs. Moritoshi Furu, Akira Nasu, Kenichi Fukiage, Seiji Otsuka, Takashi Kasahara, Tatsuya Sueyoshi, Kinya Ito, Yonghui Jin, and Hiroto Mitsui for their assistance.

This work was supported by the New Energy and Industrial Technology Development Organization (NEDO) with a project entitled Development of Evaluation Technology for Early Introduction of Regenerative Medicine, and also by the Grants-in-Aid for Scientific Research from the Japan Society for the Promotion of Science, from the Ministry of Education, Culture, Sports, Science, and Technology, and from the Ministry of Health, Labor, and Welfare.

Disclosure Statement

No competing financial interests exist.

References

1. Mankin, H.J. Nontraumatic necrosis of bone (osteonecrosis). N Engl J Med **326,** 1473, 1992.
2. Malizos, K.N., Karantanas, A.H., Varitimidis, S.E., Dailiana, Z.H., Bargiotas, K., and Maris, T. Osteonecrosis of the femoral head: etiology, imaging and treatment. Eur J Radiol **63,** 16, 2007.
3. Kaushik, A.P., Das, A., and Cui, Q. Osteonecrosis of the femoral head: an update in year 2012. World J Orthop **3,** 49, 2012.
4. Sugano, N., Atsumi, T., Ohzono, K., Kubo, T., Hotokebuchi, T., and Takaoka, K. The 2001 revised criteria for diagnosis, classification, and staging of idiopathicosteonecrosis of the femoral head. J Orthop Sci **7,** 601, 2002.
5. Ficat, R.P. Idiopathic bone necrosis of the femoral head. Early diagnosis and treatment. J Bone Joint Surg Br **67-B,** 3, 1985.

6. Hopson, C.N., and Siverhus, S.W. Ischemic necrosis of the femoral head. Treatment by core decompression. J Bone Joint Surg Am **70-A,** 1048, 1988.
7. Koo, K.H., Kim, R., Ko, G.H., Song, H.R., Jeong, S.T., and Cho, S.H. Preventing collapse in early osteonecrosis of the femoral head. A randomised clinical trial of core decompression. J Bone Joint Surg Br **77-B,** 870, 1995.
8. Sugioka, Y. Transtrochanteric anterior rotational osteotomy of the femoral head in the treatment of osteonecrosis affecting the hip: a new osteotomy operation. Clin Orthop Relat Res **130,** 191, 1978.
9. Miyanishi, K., Noguchi, Y., Yamamoto, T., Irisa, T., Suenaga, E., Jingushi, S., Sugioka, Y., and Iwamoto, Y. Prediction of the outcome of transtrochanteric rotational osteotomy for osteonecrosis of the femoral head. J Bone Joint Surg Br **82,** 512, 2000.
10. Marciniak, D., Furey, C., and Shaffer, J.W. Osteonecrosis of the femoral head. A study of 101 hips treated with vascularized fibular grafting. J Bone Joint Surg Am **87,** 742, 2005.
11. Hernigou, P., Beaujean, F., and Lambotte, J.C. Decrease in the mesenchymal stem-cell pool in the proximal femur in corticosteroid-induced osteonecrosis. J Bone Joint Surg Br **81,** 349, 1999.
12. Gangji, V., Hauzeur, J.P., Schoutens, A., Hinsenkamp, M., Appelboom, T., and Egrise, D. Abnormalities in the replicative capacity of osteoblastic cells in the proximal femur of patients with osteonecrosis of the femoral head. J Rheumatol **30,** 348, 2003.
13. Henigou, P., Bernaudin, F., Reinert, P., Kuentz, M., and Vernant, J.P. Bone marrow transplantation in sickle cell disease: effect on osteonecrosis. J Bone Joint Surg Am **79,** 1726, 1997.
14. Hernigou, P., and Beaujean, F. Treatment of osteonecrosis with autologous bone marrow grafting. Clin Orthop Relat Res **405,** 14, 2002.
15. Gangji, V., Hauzeu, J.P., Matos, C., De Maertelaer, V., Toungouz, M., and Lambermont, M. Treatment of osteonecrosis of the femoral head with implantation of autologous bone-marrow cells. A pilot study. J Bone Joint Surg Am **86-A,** 1153, 2004.
16. Gangji, V., De Maertelaer, V., and Hauzeur, J.P. Autologous bone marrow cell implantation in the treatment of non-traumatic osteonecrosis of the femoral head: Five year follow-up of a prospective controlled study. Bone **49,** 1005, 2011.
17. Caplan, A.I. Review: mesenchymal stem cells: cell-based reconstructive therapy in orthopedics. Tissue Eng **11,** 1198, 2005.
18. Steinert, A.F., Rackwitz, L., Gilbert, F., Nöth, U., and Tuan, R.S. Concise review: the clinical application of mesenchymal stem cells for musculoskeletal regeneration: current status and perspectives. Stem Cells Transl Med **1,** 237, 2012.
19. Pittenger, M.F., Mackay, A.M., Beck, S.C., Jaiswal, R.K., Douglas, R., Mosca, J.D., Moorman, M.A., Simonetti, D.W., Craig, S., and Marshak, D.R. Multilineage potential of adult human mesenchymal stem cells. Science **284,** 143, 1999.
20. Dominici, M., Le Blanc, K., Mueller, I., Slaper-Cortenbach, I., Marini, F., Krause, D., Deans, R., Keating, A., Prockop, D.J., and Horwitz, E. Minimal criteria for defining multipotent mesenchymal stromal cells. The International Society for Cellular Therapy position statement. Cytotherapy **8,** 315, 2006.
21. Casteilla, L., Planat-Bénard, V., Cousin, B., Laharrague, P., and Bourin, P. Vascular and endothelial regeneration. Curr Stem Cell Res Ther **5,** 141, 2010.
22. Zhao, D., Cui, D., Wang, B., Tian, F., Guo, L., Yang, L., Liu, B., and Yu, X. Treatment of early stage osteonecrosis of the femoral head with autologous implantation of bone marrow-derived and cultured mesenchymal stem cells. Bone **50,** 325, 2012.
23. Ikeguchi, R., Kakinoki, R., Aoyama, T., Shibata, K.R., Otsuka, S., Fukiage, K., Nishijo, K., Ishibe, T., Shima, Y., Otsuki, B., Azuma, T., Tsutsumi, S., Nakayama, T., Otsuka, T., Nakamura, T., and Toguchida, J. Regeneration of osteonecrosis of canine scapho-lunate using bone marrow stromal cells: possible therapeutic approach for Kienböck disease. Cell Transplant **15,** 411, 2006.
24. Steinberg, M.E. Classification of avascular necrosis: a comparative study. Acta Orthop Belg **65 Suppl 1,** 45, 1999.
25. Shibata, K.R., Aoyama, T., Shima, Y., Fukiage, K., Otsuka, S., Furu, M., Kohno, Y., Ito, K., Fujibayashi, S., Neo, M., Nakayama, T., Nakamura, T., and Toguchida, J. Expression of the p16INK4A gene is associated closely with senescence of human mesenchymal stem cells and is potentially silenced by DNA methylation during *in vitro* expansion. Stem Cells **25,** 2371, 2007.
26. Brothman, A.R., Persons, D.L., and Shaffer, L.G. Nomenclature evolution: changes in the ISCN from the 2005 to the 2009 edition. Cytogenet Genome Res **127,** 1, 2009.
27. Ishizaka, M., Sofue, M., Dohmae, Y., Endo, N., and Takahashi, H.E. Vascularized iliac bone graft for avascular necrosis of the femoral head. Clin Orthop Relat Res **337,** 140, 1997.
28. Leung, P.C., and Chow, Y.Y. Reconstruction of proximal femoral defects with a vascular-pedicled graft. J Bone Joint Surg Br **66-B,** 32, 1984.
29. Kuribayashi, M., Takahashi, K.A., Fujioka, M., Ueshima, K., Inoue, S., and Kubo, T. Reliability and validity of the Japanese Orthopaedic Association hip score. J Orthop Sci **15,** 452, 2010.
30. Mont, M.A., Zywiel, M.G., Marker, D.R., McGrath, M.S., and Delanois, R.E. The natural history of untreated asymptomatic osteonecrosis of the femoral head: a systematic literature review. J Bone Joint Surg Am **92-A,** 2165, 2010.
31. Nöth, U., Rackwitz, L., Steinert, A.F., and Tuan, R.S. Cell delivery therapeutics for musculoskeletal regeneration. Adv Drug Deliv Rev **62,** 765, 2010.
32. Korompilias, A.V., Lykissas, M.G., Beris, A.E., Urbaniak, J.R., and Soucacos, P.N. Vascularised fibular graft in the management of femoral head osteonecrosis: twenty years later. J Bone Joint Surg Br **91,** 287, 2009.
33. Aldridge, J.M., 3rd, Berend, K.R., Gunneson, E.E., and Urbaniak, J.R. Free vascularized fibular grafting for the treatment of postcollapse osteonecrosis of the femoral head. Surgical technique.J Bone Joint Surg **86-A Suppl 1,** 87, 2004.
34. Kawate, K., Yajima, H., Ohgushi, H., Kotobuki, N., Sugimoto, K., Ohmura, T., Kobata, Y., Shigematsu, K., Kawamura, K., Tamai, K., and Takakura, Y. Tissue-engineered approach for the treatment of steroid-induced osteonecrosis of the femoral head: transplantation of autologous mesenchymal stem cells cultured with beta-tricalcium phosphate ceramics and free vascularized fibula. Artif Organs **30,** 960, 2006.
35. Barkholt, L., Flory, E., Jekerle, V., Lucas-Samuel, S., Ahnert, P., Bisset, L., Büscher, D., Fibbe, W., Foussat, A.,

Kwa, M., Lantz, O., Mačiulaitis, R., Palomäki, T., Schneider, C.K., Sensebé, L., Tachdjian, G., Tarte, K., Tosca, L., and Salmikangas, P. Risk of tumorigenicity in mesenchymal stromal cell-based therapies-Bridging scientific observations and regulatory viewpoints. Cytotherapy **15,** 753, 2013.

36. Rubio, D., Garcia-Castro, J., Martín, M.C., de la Fuente, R., Cigudosa, J.C., Lloyd, A.C., and Bernad, A. Spontaneous human adult stem cell transformation. Cancer Res **65,** 3035, 2005.
37. Røsland, G.V., Svendsen, A., Torsvik, A., Sobala, E., McCormack, E., Immervoll, H., Mysliwietz, J., Tonn, J.C., Goldbrunner, R., Lønning, P.E., Bjerkvig, R., and Schichor, C. Long-term cultures of bone marrow-derived human mesenchymal stem cells frequently undergo spontaneous malignant transformation. Cancer Res **69,** 5331, 2009.
38. de la Fuente, R., Bernad, A., Garcia-Castro, J., Martin, M.C., and Cigudosa, J.C. Retraction: spontaneous human adult stem cell transformation. Cancer Res **70,** 6682, 2010.
39. Garcia, S., Bernad, A., Martín, M.C., Cigudosa, J.C., Garcia-Castro, J., and de la Fuente, R. Pitfalls in spontaneous *in vitro* transformation of human mesenchymal stem cells. Exp Cell Res **316,** 1648, 2010.
40. Torsvik, A., Røsland, G.V., Svendsen, A., Molven, A., Immervoll, H., McCormack, E., Lønning, P.E., Primon, M., Sobala, E., Tonn, J.C., Goldbrunner, R., Schichor, C., Mysliwietz, J., Lah, T.T., Motaln, H., Knappskog, S., and Bjerkvig, R. Spontaneous malignant transformation of human mesenchymal stem cells reflects cross-contamination: putting the research field on track - letter. Cancer Res **70,** 6393, 2010.
41. Sensebé, L., Bourin, P., and Tarte, K. Good manufacturing practices production of mesenchymal stem/stromal cells. Hum Gene Ther **22,** 19, 2011.
42. Tarte, K., Gaillard, J., Lataillade, J.J., Fouillard, L., Becker, M., Mossafa, H., Tchirkov, A., Rouard, H., Henry, C., Splingard, M., Dulong, J., Monnier, D., Gourmelon, P., Gorin, N.C., Sensebé, L.; Société Française de Greffe de Moelle et Thérapie Cellulaire. Clinical-grade production of human mesenchymal stromal cells: occurrence of aneuploidy without transformation. Blood **115,** 1549, 2010.
43. Kondo, N., Ogose, A., Tokunaga, K., Ito, T., Arai, K., Kudo, N., Inoue, H., Irie, H., and Endo, N. Bone formation and resorption of highly purified beta-tricalcium phosphate in the rat femoral condyle. Biomaterials **26,** 5600, 2005.
44. Nasu, T., Takemoto, M., Akiyama, N., Fujibayashi, S., Neo, M., and Nakamura, T. EP4 agonist accelerates osteoinduction and degradation of beta-tricalcium phosphate by stimulating osteoclastogenesis. J Biomed Mater Res **A89,** 601, 2009.
45. Doorn, J., Moll, G., Le Blanc, K., van Blitterswijk, C., and de Boer, J. Therapeutic applications of mesenchymal stromal cells: paracrine effects and potential improvements. Tissue Eng Part B Rev **18,** 101, 2012.
46. Wang, J., Liao, L., and Tan, J. Mesenchymal-stem-cell-based experimental and clinical trials: current status and open questions. Expert Opin Biol Ther **11,** 893, 2011.

Address correspondence to:
Junya Toguchida, MD, PhD
Department of Tissue Regeneration
Institute for Frontier Medical Sciences
Kyoto University
53 Kawahara-cho, Shogoin, Sakyo-ku
Kyoto 606-8507
Japan

E-mail: togjun@frontier.kyoto-u.ac.jp

Received: February 3, 2014
Accepted: February 18, 2014
Online Publication Date: April 4, 2014

Osteoarthritis and Cartilage 22 (2014) 1036–1043

Osteoarthritis and Cartilage

OARSI OSTEOARTHRITIS RESEARCH SOCIETY INTERNATIONAL

Destabilization of the medial meniscus leads to subchondral bone defects and site-specific cartilage degeneration in an experimental rat model

H. Iijima †, T. Aoyama ‡, A. Ito †, J. Tajino †, M. Nagai †, X. Zhang †, S. Yamaguchi †, H. Akiyama §, H. Kuroki † *

† *Department of Motor Function Analysis, Human Health Sciences, Graduate School of Medicine, Kyoto University, Japan*
‡ *Department of Development and Rehabilitation of Motor Function, Human Health Sciences, Graduate School of Medicine, Kyoto University, Japan*
§ *Department of Orthopaedic Surgery, Graduate School of Medicine, Gifu University, Japan*

ARTICLE INFO

Article history:
Received 20 February 2014
Accepted 7 May 2014

Keywords:
Destabilization of medial meniscus
Subchondral bone defects
Cartilage degeneration
Cartilage covered by menisci

SUMMARY

Objective: This study aimed to investigate subchondral bone changes using micro-computed tomography (micro-CT) and regional differences in articular cartilage degeneration, focusing on changes of cartilage covered by menisci, in the early phase using a destabilization of the medial meniscus (DMM) model.
Method: The DMM model was created as an experimental rat osteoarthritis (OA) model (12 weeks old; $n = 24$). At 1, 2, and 4 weeks after surgery, the rats were sacrificed, and knee joints were scanned using a Micro-CT system. Histological sections of the medial tibial plateau, which was divided into inner, middle, and outer regions, were prepared and scored using the modified OARSI scoring system. The cartilage thickness was also calculated, and matrix metalloproteinase 13 (MMP13), Col2-3/4c, and vascular endothelial growth factor (VEGF) expression was assessed immunohistochemically.
Results: Subchondral bone defects were observed in the middle region, in which the cartilage thickness decreased over time after surgery, and these defects were filled with MMP13- and VEGF-expressing fibrous tissue. The OARSI score increased over time in the middle region, and the score was significantly higher in the middle region than in the inner and outer regions at 1, 2, and 4 weeks after surgery. Col2-3/4c and MMP13 expression was observed primarily in the meniscus-covered outer region, in which the cartilage thickness increased over time.
Conclusion: Loss of meniscal function caused cartilage degeneration and subchondral bone defects in the early phase site-specifically in the middle region. Furthermore, our results might indicate cartilage covered by menisci is easily degraded resulting in osmotic swelling of the cartilage in early OA.

Introduction

Osteoarthritis (OA) is the most common form of arthritis and a major cause of pain[1] and disability[2] in older adults. The common risk factors for knee OA include age, sex, obesity, prior joint injury, and mechanical factors, including malalignment and abnormal joint kinematics during ambulation[3]. Despite the multifactorial nature of knee OA, the mechanical environment of the knee during ambulation has a profound influence on the initiation and progression of knee OA[4]. The increased incidence of medial compartment knee OA is therefore believed to result from higher mechanical loading of the medial compartment.

The menisci play an important role in load-bearing distribution at the knee[5]. Loss of meniscal function due to meniscal extrusion and meniscectomy result in increased mechanical loading of the articular cartilage and subchondral bone of the affected knee[6,7]. Total meniscectomy increases the risk of initiation and progression of knee OA radiographically by 14-fold after 21 years[8]. However, the initiating events in knee OA after the loss of meniscal function remain unknown.

* Address correspondence and reprint requests to: H. Kuroki, Department of Motor Function Analysis, Human Health Sciences, Graduate School of Medicine, Kyoto University, 53 Shogoin, Kawahara-cho, Sakyo-ku, Kyoto 606-8507, Japan. Tel: 81-75-751-3963; Fax: 81-75-751-3909.
E-mail addresses: iijima.hirotaka.75s@st.kyoto-u.ac.jp (H. Iijima), aoyama.tomoki.4e@kyoto-u.ac.jp (T. Aoyama), ito.akira.27n@st.kyoto-u.ac.jp (A. Ito), tajino.junichi.57z@st.kyoto-u.ac.jp (J. Tajino), nagai.momoko.36v@st.kyoto-u.ac.jp (M. Nagai), zhang.xiangkai.48v@st.kyoto-u.ac.jp (X. Zhang), yamaguchi.shouki.26n@st.kyoto-u.ac.jp (S. Yamaguchi), hakiyama@kuhp.kyoto-u.ac.jp (H. Akiyama), kuroki.hiroshi.6s@kyoto-u.ac.jp (H. Kuroki).

http://dx.doi.org/10.1016/j.joca.2014.05.009
1063-4584/

Recently, subchondral bone changes are determined to play an important role in the pathogenesis of knee OA[9,10]. In human studies, subchondral bone fracture frequently occurs after meniscectomy, worsening the patient's clinical condition[11–13]. Additionally, meniscal extrusion is associated to increase subchondral bone cyst[7]. However, whether these subchondral bone changes occur in early phase after loss of meniscal function are still unknown. Therefore, understanding of the subchondral bone changes in the early phase after loss of meniscal function is important for preventing the initiation and progression of knee OA.

An experimental OA model of surgical destabilization of the medial meniscus (DMM) has been used for common knee OA basic research[14]. Previous studies showed subchondral bone changes by histological methods after DMM[15–17]. Recently, extensive micro-computed tomography (micro-CT) studies which observed morphological changes of subchondral bone in a rat OA model have been conducted[9,18]. Also in DMM rat model, trabecular porosity was increased in 4 weeks after surgery by micro-CT study[19], however the time-course of subchondral bone changes in early phase after DMM is still unknown.

DMM results in an elevation of peak local contact stress in the medial compartment[20,21] and even changes the distribution of mechanical loading in menisci-covered and uncovered cartilage. In recent *ex vivo* studies, cartilage covered by menisci differed from uncovered cartilage in terms of histology[22,23], mechanical properties[22–24], and metabolic activities[25]. These studies indicated cartilage covered by menisci is potentially susceptive to mechanical loading than cartilage uncovered by menisci. Some animal studies indicated that the kinetics of cartilage degeneration differ between these two regions[24,26,27], and cartilage covered by menisci displays greater degeneration after meniscectomy than uncovered cartilage[28]. However the time-course change and regional change of cartilage especially cartilage covered by menisci after loss of meniscal function are still unclear.

The first purpose of this study was to investigate subchondral bone changes over time after loss of meniscal function using micro-CT and the second was to investigate regional differences in articular cartilage degeneration, focusing on changes of cartilage covered by menisci, in the early phase using a DMM model.

Method

Experimental animals and surgical procedures

This study was approved by the animal research committee of Kyoto University (approval number: 13602). An experimental OA model was created *via* DMM[14] in male Wistar rats (12 weeks old; $n = 24$; mean body weight, 272.4 g). After the rats were anesthetized by 8.5 ml/kg somnopentyl, the right knee joint was exposed following a medial capsular incision and gentle lateral displacement of the knee extensor muscles without transection of the patellar ligament. Then, the medial meniscotibial ligament (MMTL) was transected, and the medial meniscus could be displaced medially. After replacement of the extensor muscles, the medial capsular incision was sutured, and the skin was closed. A sham operation was performed on the left knee joint using the same approach without MMTL transection. The animals were then permitted unrestricted activity and provided free access to food and water.

Micro-CT analysis of the subchondral bone

At 1, 2, and 4 weeks after surgery ($n = 8$ for each time point), the rats were sacrificed, and knee joints were scanned using a Micro-CT system (SMX-100CT, Shimadzu, Kyoto, Japan) at voxel size 21 μm resolution. After scanning, the knee joint was three-dimensionally reconstructed using a software package (Amira5.4, Visage, Berlin, Germany). Changes of the subchondral bone were observed in the sagittal and frontal sections qualitatively.

Histological analysis

The knee joints were fixed in 4% paraformaldehyde overnight and decalcified in 10% EDTA. The samples were dehydrated and embedded in paraffin. Paraffin sections were prepared from the medial tibial plateau in the frontal plane according to previously described methods[29] and alternately stained with hematoxylin-eosin (H-E) and toluidine blue. The toluidine blue-stained sections were evaluated using the OARSI score established by Pritzker *et al.*[30], which scores the product of six grades (depth of lesion) and four stages (extent of involvement) on a scale of 0 (normal) to 24 (severe OA). To detect regional differences in cartilage, the method was slightly modified such that the cartilage of the medial tibia was divided into outer, middle, and inner regions, each comprising approximately one-third of the total arc length[31,32]. The cartilage in the outer regions is covered by the meniscus, whereas the cartilage in middle and inner region is not covered by the meniscus. To assess cartilage thickness, the frontal sections were used for thickness histomorphometric analysis, and digital images of each region (×40) were captured. The cartilage thickness of each region was defined as the mean value of three thickness measurements performed at regular intervals perpendicular to the cartilage surface[33] in the photo image of histology using the Image-J software.

Immunohistochemistry

Immunohistochemical staining of vascular endothelial growth factor (VEGF), matrix metalloproteinase 13 (MMP13), and Col2-3/4c was performed. Col2-3/4C antibody was kindly donated by Dr A.R. Pool (Shriners Hospitals for Children, Department of Surgery, McGill University, Montreal). The Col2-3/4C antibody is a rabbit polyclonal antibody directed against the COOH terminus of the three-quarter fragment. It is generated specifically *via* cleavage of native type II collagen by mammalian collagenases. Deparaffinized sections were treated with 0.3% hydrogen peroxide to reduce endogenous peroxidase activity. Then, the sections were treated with 1.25 (anti-VEGF) or 0.6% (anti-MMP13) hyaluronidase (Sigma–Aldrich Co., St Louis, MO, USA) in PBS for 60 min at room temperature and 1% hyaluronidase in PBS for 30 min at 37°C (Col2-3/4c). Non-specific staining was blocked by incubation of the sections with 5 (anti-VEGF) or 10% (anti-MMP13, Col2-3/4c) normal goat serum for 60 min.

Subsequently, the sections were treated with anti-VEGF (diluted 1:50), anti-MMP13 (diluted 1:1000), and Col2-3/4c (diluted 1:800) and further incubated overnight at 4°C. Detection was performed using the streptavidin-biotin-peroxidase complex technique with an Elite ABC kit (diluted 1:100; Vector Laboratories, Burlingame, CA, USA). Immunoreactivity was visualized by incubation with diaminobenzidine solution (Vector Laboratories) followed by counterstaining with hematoxylin. The primary antibody was not added to negative controls.

Statistical analysis

The software program JMP 11 (SAS Institute, Cary, NC USA) was used for the statistical analysis. Descriptive statistics were calculated as median and interquartile range for OARSI score and as means and 95% confidence intervals (CIs) for cartilage thickness. The Mann–Whitney U test was used for pair-wise differences of OARSI score and the paired t-test was used for pair-wise differences

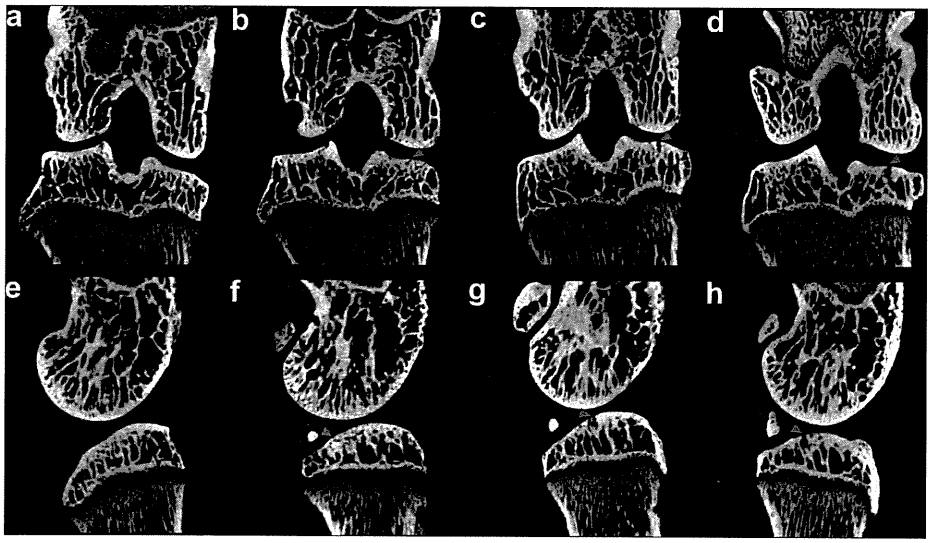

Fig. 1. Micro-CT images of the subchondral bone in 1 week (b, f), 2 weeks (c, g), and 4 weeks (d, h) after DMM surgery. Subchondral bone defects were confirmed in the middle region of the medial tibia in the frontal sections (b–d) and posterior regions of the sagittal sections (f–h) after DMM surgery. No subchondral bone defects were confirmed in 4 weeks after sham surgery (a, e).

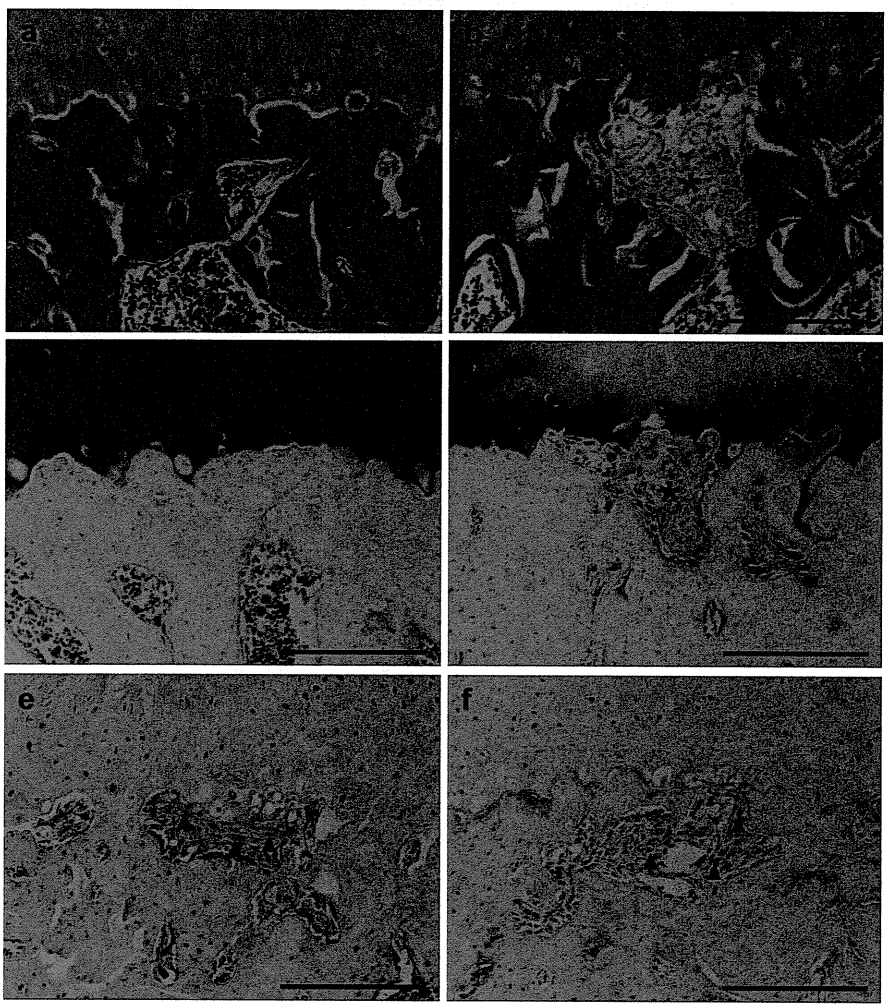

Fig. 2. Histological findings of the subchondral bone defects on micro-CT image in 4 weeks after surgery. HE and toluidine blue staining in sham (a, c) and DMM cartilage (b, d). Subchondral bone defects in DMM cartilage were filled with fibrous tissue (asterisk). Immunohistochemical analysis of VEGF (e) and MMP13 (f) expression in DMM cartilage. VEGF-positive and MMP13-positive cells were confirmed in the fibrous tissue (arrowhead). Magnification, ×200. *Scale bars* = 200 μm.

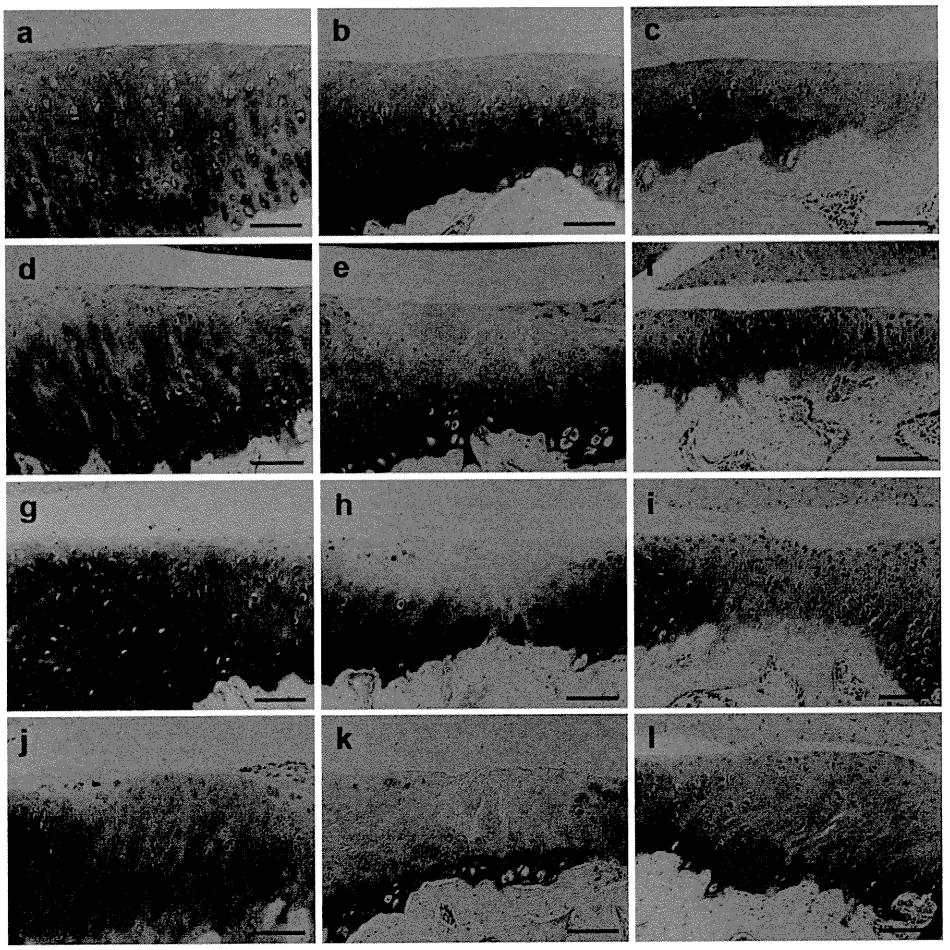

Fig. 3. Toluidine blue staining of the cartilage in the inner, middle, and outer regions of the medial tibia in 1 week (d–f), 2 weeks (g–i), and 4 weeks (j–l) after DMM surgery. In the inner region, there were no pronounced change of the cartilage in experimental periods (d, g, j). In the middle region, matrix loss in the upper one-third of the cartilage and vertical fissures were confirmed in 1 week (e). The matrix loss further progressed into the upper two-thirds of the cartilage in 2 and 4 weeks (h, k). In the outer region, chondrocyte proliferation and clustering were confirmed (arrowhead) without cartilage degeneration in 1 week (f). Cartilage thickness was increased together with matrix production in 2 weeks (i); however, chondrocyte numbers were decreased, and the surface was irregular in 4 weeks (l). No cartilage degeneration were confirmed in 4 weeks after sham surgery (a–c). Magnification, ×100. *Scale bars* = 100 μm.

of cartilage thickness. In all cases, $P < 0.05$ was considered significant.

Results

Subchondral bone changes

Subchondral bone defects were observed in the middle region 1, 2, and 4 weeks after DMM surgery on micro-CT images (Fig. 1). These defects were observed in the center of thickened subchondral bone and the destruction were exacerbated over time. According to the histological findings, these defects were filled with fibrous tissue [Fig. 2(a and c)]. The immunohistochemical localization of VEGF and MMP13 was observed in the fibrous tissue [Fig. 2(e and f)].

Histological findings

The most severe lesions were confined to the middle region of the medial tibia in DMM cartilage [Fig. 3(e, h and k)]. Vertical fissures with matrix loss in the upper third of the cartilage were confirmed beginning 1 week after DMM surgery [Fig. 3(e)]. Matrix loss had worsened by 4 weeks after surgery, indicating depletion of the matrix in the upper two third of the cartilage with chondrocyte loss [Fig. 3(h and k)]. Meanwhile, chondrocyte proliferation and matrix production were confirmed in the meniscus-covered outer region, which did not display extensive cartilage degeneration [Fig. 3(f, i and l)].

The result of OARSI score was shown in Fig. 4. The OARSI score was increased locally in the middle region [Fig. 4(b)] of DMM over time and significantly higher than sham at all periods (1 week: 7.5[2.3–8.0] vs 0[0–1.0]; 2 weeks: 12.0[7.5–13.1] vs 0[0–0]; 4 weeks: 13.8 [12.4–16.0] vs 0[0–0]). In outer region [Fig. 4(c)], the OARSI score was slightly increased over time and significantly higher than sham at all periods though changes was not as high as in middle region (1 week: 3.0[2.0–3.0] vs 0[0–1.0]; 2 weeks: 3.0[3.0–3.8] vs 0[0–0]; 4 weeks: 4.0[3.3–6.0] vs 0[0–0]). There were no pronounced change of the OARSI score in inner region [Fig. 4(a)] and significantly higher than sham only in 4 weeks (1 week: 1.0[0.3–1.0] vs 0[0–0.8]; 2 weeks: 1.0 [1.0–1.8] vs 0.5[0–1.0]; 4 weeks: 1.0[1.0–5.5] vs 0[0–1.0]). The OARSI in the middle region was significantly higher than in the inner and outer regions at 1, 2, and 4 weeks after surgery (data not shown).

The cartilage thickness of DMM increased over time in the outer region (1.5-fold in 4 weeks), whereas that of DMM decreased over

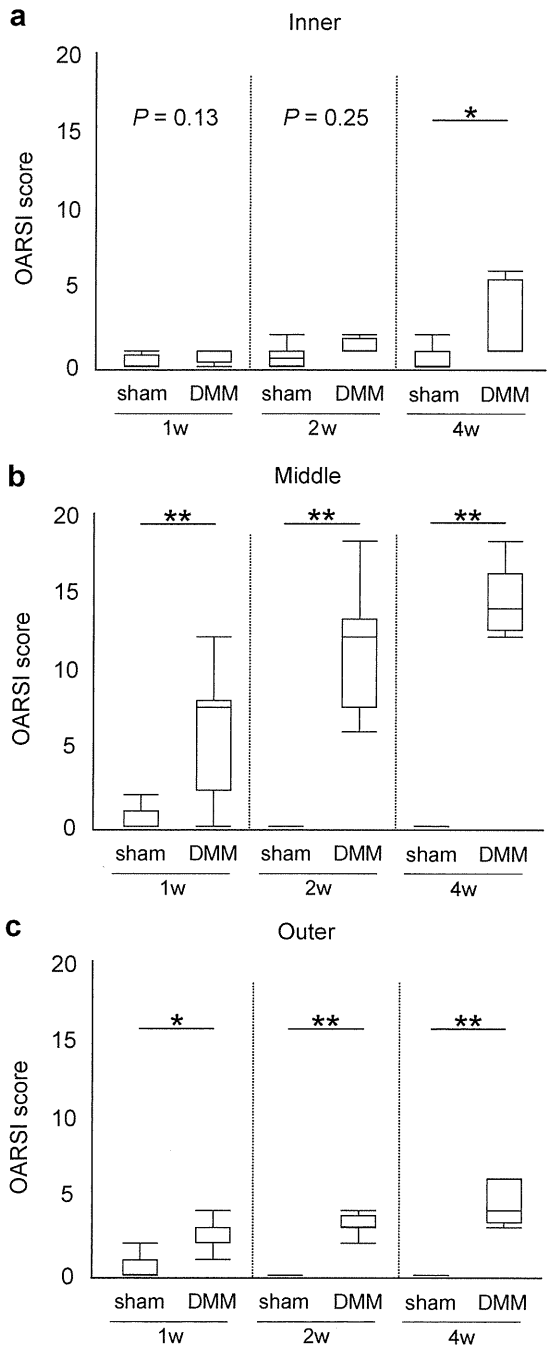

Fig. 4. Time-course of changes in the OARSI score in inner (a), middle (b), and outer region (c). OARSI scores increased, particularly in the middle region, over time after DMM surgery, whereas slight increases in the OARSI score was noted in the outer regions. Boxplots displaying median values and interquartile range ($n = 8$; $^{*}P < 0.05$; $^{**}P < 0.01$ by Mann–Whitney U test).

time in the middle region (0.8-fold in 4 weeks) (Fig. 5). In inner region, cartilage thickness of DMM and sham was slightly increased in 2 weeks following slightly decreased in 4 weeks, however there were no significantly differences between DMM and sham [Fig. 5(a)]. Cartilage thickness of middle region was significantly thinner than sham in 4 weeks [Fig. 5(b)] and that of outer region was significantly thicker than sham in 1, 2, and 4 weeks [Fig. 5(c)].

Type II collagen degradation in the inner, middle, and outer regions

Collagenase cleavage sites were present together with surface fibrillation in the inner and middle regions at 4 weeks [Fig. 6(d and e)]. Interestingly, in the outer region, collagenase cleavage sites were present in all layers [Fig. 6(f)]. In sham cartilage, collagenase cleavage sites were present only on the surface of the inner region [Fig. 6(a–c)].

MMP13 was also present together with surface fibrillation in the inner and middle regions after 4 weeks [Fig. 7(d and e)] and in all

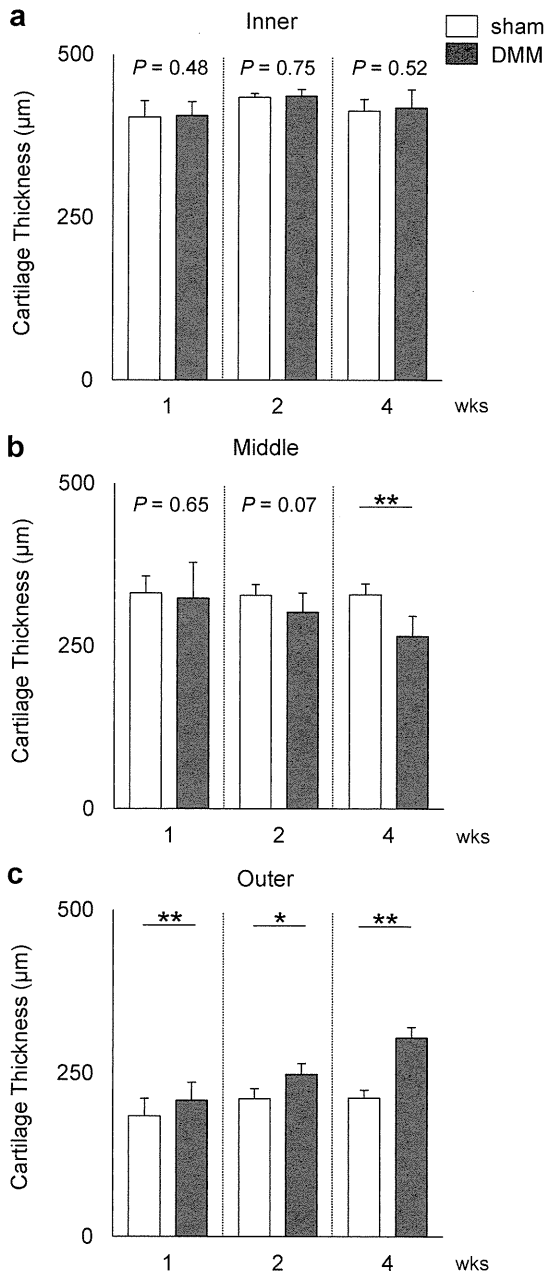

Fig. 5. Time-course of changes in the cartilage thickness in inner (a), middle (b), and outer region (c). Cartilage thickness of middle region became thinner over time whereas that of outer region became thicker over time. Bars show the mean ± 95% CIs ($n = 8$; $^{*}P < 0.05$; $^{**}P < 0.01$ by paired t-test).

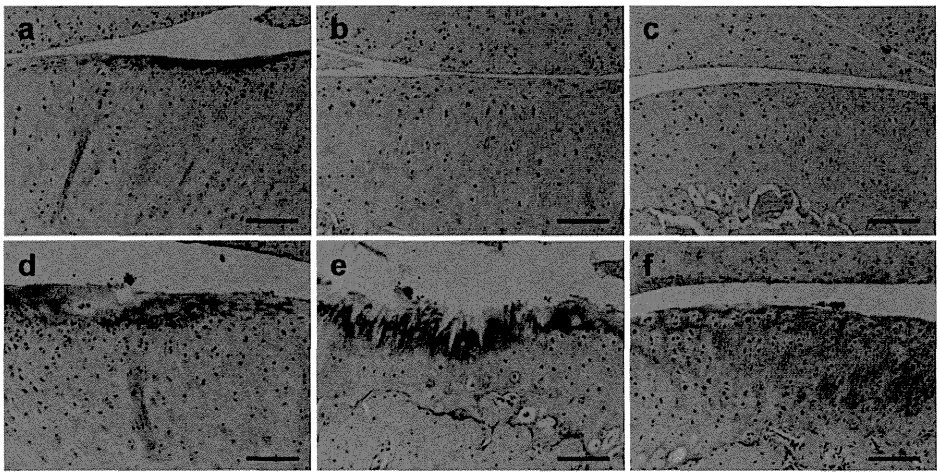

Fig. 6. Immunohistochemical staining of Col2-3/4c in sham (a–c) and DMM cartilage (d–f) in 4 weeks after surgery. Inner (a, d), middle (b, e), and outer cartilage (c, f). In DMM cartilage, Col2-3/4c staining was confirmed on the surface in the inner (d) and middle regions (e), in which fibrillation was observed. In the outer region of the OA cartilage, Col2-3/4c staining was confirmed in most layers, whereas only slight fibrillation was observed (f). Only a part of the surface of the inner region was positively stained for Col2-3/4c in sham cartilage (a). Magnification, ×100. *Scale bars* = 100 μm.

layers of the outer region [Fig. 7(f)]. In sham cartilage, MMP13 was present only on the surface in the inner region [Fig. 7(a–c)].

Discussion

In this study, subchondral bone defects were observed site-specifically in middle region in micro-CT images, and these were not repaired by 4 weeks after DMM surgery (Fig. 1). These findings were consistent with previous studies using collagenase-injected model[34] and ACLT model[18]. Although we could not confirm what caused subchondral bone cyst, Landells proposed the presence of a breached subchondral bone plate was the source of subchondral bone cyst formation[35]. Degenerated cartilage lost the ability to maintain fluid pressurization, resulting in the transmission of excessive mechanical loading and exudation of pressurized fluid into the breached underlying bone which might lead to subsequent cyst expansion[9,36]. Furthermore, previous studies showed cystic tissue in OA subchondral bone is capable of activating higher numbers of osteoclasts[34,37,38]. These findings indicated subchondral bone cyst might be the results of osteoclast activity drilling holes towards the cartilage.

We also revealed that subchondral bone defects corresponded with cartilage degeneration and cartilage thinning at the site of greatest disease severity, which agrees with previous findings in humans[39,40] and animal models[9]. Cartilage thinning in the middle region results in extreme mechanical loading under the subchondral bone plate of the middle region during ambulation. Chronic abnormal mechanical loading after meniscal extrusion might cause repetitive microtraumas in the trabeculae, leading to angiogenesis, subchondral bone remodeling and stress-induced bone resorption.

Defects in subchondral bone were filled with fibrous tissue, which expressed MMP13 and communicated with cartilage in the osteochondral junction [Fig. 2(f)]. MMP13 degrades type II collagen

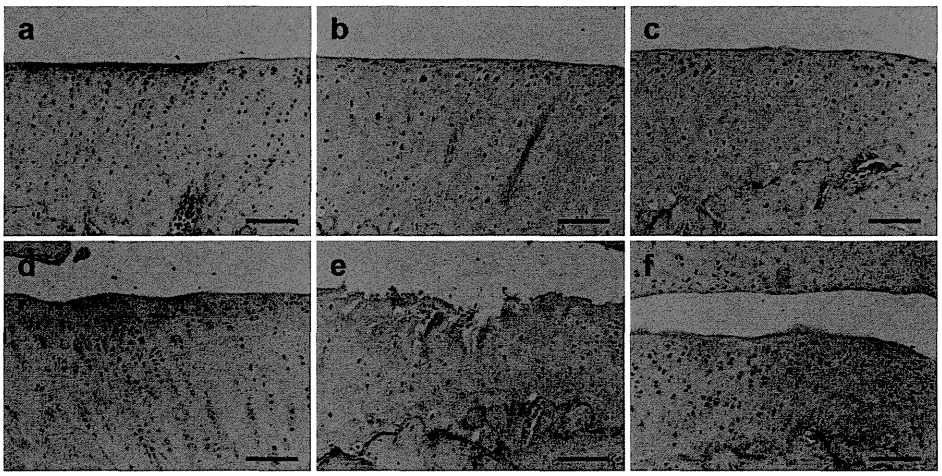

Fig. 7. Immunohistochemical staining of MMP13 in sham (a–c) and DMM cartilage (d–f) in 4 weeks after surgery. Inner (a, d), middle (b, e), and outer cartilage (c, f). In DMM cartilage, MMP13 expression was confirmed on the surface in the inner (d) and middle regions (e), in which fibrillation was observed. Similar to Col2-3/4c staining in the outer region, MMP13 expression was confirmed in nearly all layers (f). Only a part of the surface of the inner region in the sham cartilage displayed positive MMP13 staining (a). Magnification, ×100. *Scale bars* = 100 μm.

specifically, and it is associated with the progression of knee OA[41]. As activated osteoblasts in subchondral bone cysts expressed MMP1[40], MMPs might contribute to absorb both the bone and articular matrix.

The increased cartilage thickness in the meniscus-covered outer region is similar to the findings of previous studies[31,33]. Peripheral thickening might be an adaptive or compensatory mechanism to increase the articular cartilage area of contact[42]. From our findings, however, the cartilage of the outer region might have failed to adapt to mechanical loading because MMP13 expression and type II collagen cleavage were confirmed in all layers (Figs. 6 and 7), resulting in other pathologic changes in cartilage, such as cyst formation (Supplementary Figure)[43]. Cartilage covered by menisci receives mechanical loading *via* menisci under normal conditions, and it has less cartilage matrix than uncovered cartilage[22,23]. Therefore, the outer region displayed destructive changes in response to direct mechanical loading after the loss of meniscal function which easily resulting in osmotic swelling of the cartilage (Fig. 3).

The limitations of the study should be mentioned. First, it remains unclear whether subchondral bone defects were first initiated by the loss of cartilage integrity or because of a subchondral bone failure. Second, the experimental period was only 1, 2, and 4 weeks after surgery; therefore, the long-term changes in cartilage and subchondral bone are unknown. Third, we use an experiment model of rats, and thus, our findings might not translate directly to humans, as anatomical differences between rats and humans may affect the extent of cartilage degeneration.

In conclusion, the loss of meniscal function resulted in cartilage degeneration and subchondral bone defects in the early phase site-specifically in the middle region. Additionally, fibrous tissue in areas of subchondral bone defects expressed MMP13, indicating osteochondral changes in early OA. Collagenase cleavage sites and MMP13 were most commonly present in the outer region covered by menisci, which thickened over time after surgery. Our results might indicate cartilage covered by menisci is easily degraded resulting in osmotic swelling of the cartilage in early OA.

Author contributions

All authors have made substantial contributions to (1) the conception and design of the study, or acquisition of data, or analysis and interpretation of data; (2) drafting the article or revising it critically for important intellectual content; and (3) final approval of the version to be submitted.

The specific contributions of the authors are as follows:

(1) Conception and design of the study: HI, TA, AI, MN, XZ, SY, HA, HK
(2) Analysis and interpretation of the data: HI, TA, AI, MN, XZ, SY, HK
(3) Drafting of the article: HI, TA, JT, HK
(4) Critical revision of the article for important intellectual content: HI, TA, AI, HA, HK
(5) Final approval of the article: HI, TA, HK
(6) Statistical expertise: HI, TA, JT
(7) Obtaining of funding: HK
(8) Collection and assembly of data: HI

Role of the funding source

This study was supported in part by a JSPS KAKENHI Grant-in-Aid for Scientific Research (A) (number 20240057) and a JSPS KAKENHI Grant-in-Aid for Challenging Exploratory Research (number 25560258).

Conflict of interest

The authors have no competing interests.

Acknowledgments

The authors thank Dr A.R. Pool (Shriners Hospitals for Children, Department of Surgery, McGill University, Montreal) for the generous gift of the Col2-3/4C antibody, which made a large contribution to our new findings.

Supplementary data

Supplementary data related to this article can be found at http://dx.doi.org/10.1016/j.joca.2014.05.009.

References

1. Muraki S, Oka H, Akune T, Mabuchi A, En-yo Y, Yoshida M, *et al.* Prevalence of radiographic knee osteoarthritis and its association with knee pain in the elderly of Japanese population-based cohorts: the ROAD study. Osteoarthritis Cartilage 2009;17:1137–43.
2. Liu L, Ishijima M, Kaneko H, Futami I, Sadatsuki R, Hada S, *et al.* Disability for daily living is a predictor for joint replacement in patients with end-stage knee osteoarthritis. J Bone Miner Metab 2013;32:192–9.
3. Blagojevic M, Jinks C, Jeffery A, Jordan KP. Risk factors for onset of osteoarthritis of the knee in older adults: a systematic review and meta-analysis. Osteoarthritis Cartilage 2010;18:24–33.
4. Andriacchi TP, Koo S, Scanlan SF. Gait mechanics influence healthy cartilage morphology and osteoarthritis of the knee. J Bone Joint Surg Am 2009;91(Suppl 1):95–101.
5. Messner K, Gao J. The menisci of the knee joint. Anatomical and functional characteristics, and a rationale for clinical treatment. J Anat 1998;193:161–78.
6. Lee SJ, Aadalen KJ, Malaviya P, Lorenz EP, Hayden JK, Farr J, *et al.* Tibiofemoral contact mechanics after serial medial meniscectomies in the human cadaveric knee. Am J Sports Med 2006;34:1334–44.
7. Wang Y, Wluka AE, Pelletier JP, Martel-Pelletier J, Abram F, Ding C, *et al.* Meniscal extrusion predicts increases in subchondral bone marrow lesions and bone cysts and expansion of subchondral bone in osteoarthritic knees. Rheumatology 2010;49:997–1004.
8. Roos H, Lauren M, Adalberth T, Roos EM, Jonsson K, Lohmander LS. Knee osteoarthritis after meniscectomy: prevalence of radiographic changes after twenty-one years, compared with matched controls. Arthritis Rheum 1998;41:687–93.
9. McErlain DD, Ulici V, Darling M, Gati JS, Pitelka V, Beier F, *et al.* An in vivo investigation of the initiation and progression of subchondral cysts in a rodent model of secondary osteoarthritis. Arthritis Res Ther 2012;14:R26.
10. Castaneda S, Roman-Blas JA, Largo R, Herrero-Beaumont G. Subchondral bone as a key target for osteoarthritis treatment. Biochem Pharmacol 2012;83:315–23.
11. Higuchi H, Kobayashi Y, Kobayashi A, Hatayama K, Kimura M. Histologic analysis of postmeniscectomy osteonecrosis. Am J Orthop 2013;42:220–2.
12. Nakamura N, Horibe S, Nakamura S, Mitsuoka T. Subchondral microfracture of the knee without osteonecrosis after arthroscopic medial meniscectomy. Arthroscopy 2002;18:538–41.

13. MacDessi SJ, Brophy RH, Bullough PG, Windsor RE, Sculco TP. Subchondral fracture following arthroscopic knee surgery. A series of eight cases. J Bone Joint Surg Am 2008;90:1007–12.
14. Glasson SS, Blanchet TJ, Morris EA. The surgical destabilization of the medial meniscus (DMM) model of osteoarthritis in the 129/SvEv mouse. Osteoarthritis Cartilage 2007;15:1061–9.
15. Loeser RF, Olex AL, McNulty MA, Carlson CS, Callahan M, Ferguson C, *et al.* Disease progression and phasic changes in gene expression in a mouse model of osteoarthritis. PLoS One 2013;8:e54633.
16. Ruan MZ, Dawson B, Jiang MM, Gannon F, Heggeness M, Lee BH. Quantitative imaging of murine osteoarthritic cartilage by phase-contrast micro-computed tomography. Arthritis Rheum 2013;65:388–96.
17. Botter SM, Glasson SS, Hopkins B, Clockaerts S, Weinans H, van Leeuwen JP, *et al.* ADAMTS5-/- mice have less subchondral bone changes after induction of osteoarthritis through surgical instability: implications for a link between cartilage and subchondral bone changes. Osteoarthritis Cartilage 2009;17:636–45.
18. McErlain DD, Appleton CT, Litchfield RB, Pitelka V, Henry JL, Bernier SM, *et al.* Study of subchondral bone adaptations in a rodent surgical model of OA using in vivo micro-computed tomography. Osteoarthritis Cartilage 2008;16:458–69.
19. Gu XI, Palacio-Mancheno PE, Leong DJ, Borisov YA, Williams E, Maldonado N, *et al.* High resolution micro arthrography of hard and soft tissues in a murine model. Osteoarthritis Cartilage 2012;20:1011–9.
20. Kenny C. Radial displacement of the medial meniscus and Fairbank's signs. Clin Orthop Relat Res 1997;339:163–73.
21. Arunakul M, Tochigi Y, Goetz JE, Diestelmeier BW, Heiner AD, Rudert J, *et al.* Replication of chronic abnormal cartilage loading by medial meniscus destabilization for modeling osteoarthritis in the rabbit knee in vivo. J Orthop Res 2013;31:1555–60.
22. Thambyah A, Nather A, Goh J. Mechanical properties of articular cartilage covered by the meniscus. Osteoarthritis Cartilage 2006;14:580–8.
23. Iijima H, Aoyama T, Ito A, Tajino J, Nagai M, Zhang X, *et al.* Immature articular cartilage and subchondral bone covered by menisci are potentially susceptive to mechanical load. BMC Musculoskelet Disord 2014;15:101.
24. Yeow CH, Lau ST, Lee PV, Goh JC. Damage and degenerative changes in menisci-covered and exposed tibial osteochondral regions after simulated landing impact compression-a porcine study. J Orthop Res 2009;27:1100–8.
25. Bevill SL, Briant PL, Levenston ME, Andriacchi TP. Central and peripheral region tibial plateau chondrocytes respond differently to in vitro dynamic compression. Osteoarthritis Cartilage 2009;17:980–7.
26. Stoop R, Buma P, van der Kraan PM, Hollander AP, Clark Billinghurst R, Robin Poole A, *et al.* Differences in type II collagen degradation between peripheral and central cartilage of rat stifle joints after cranial cruciate ligament transection. Arthritis Rheum 2000;43:2121–31.
27. Young AA, McLennan S, Smith MM, Smith SM, Cake MA, Read RA, *et al.* Proteoglycan 4 downregulation in a sheep meniscectomy model of early osteoarthritis. Arthritis Res Ther 2006;8:R41.
28. Cake MA, Read RA, Corfield G, Daniel A, Burkhardt D, Smith MM, *et al.* Comparison of gait and pathology outcomes of three meniscal procedures for induction of knee osteoarthritis in sheep. Osteoarthritis Cartilage 2013;21:226–36.
29. Gerwin N, Bendele AM, Glasson S, Carlson CS. The OARSI histopathology initiative – recommendations for histological assessments of osteoarthritis in the rat. Osteoarthritis Cartilage 2010;18:S24–34.
30. Pritzker KP, Gay S, Jimenez SA, Ostergaard K, Pelletier JP, Revell PA, *et al.* Osteoarthritis cartilage histopathology: grading and staging. Osteoarthritis Cartilage 2006;14:13–29.
31. Cake MA, Read RA, Guillou B, Ghosh P. Modification of articular cartilage and subchondral bone pathology in an ovine meniscectomy model of osteoarthritis by avocado and soya unsaponifiables (ASU). Osteoarthritis Cartilage 2000;8:404–11.
32. Little CB, Smith MM, Cake MA, Read RA, Murphy MJ, Barry FP. The OARSI histopathology initiative – recommendations for histological assessments of osteoarthritis in sheep and goats. Osteoarthritis Cartilage 2010;18:S80–92.
33. Thote T, Lin AS, Raji Y, Moran S, Stevens HY, Hart M, *et al.* Localized 3D analysis of cartilage composition and morphology in small animal models of joint degeneration. Osteoarthritis Cartilage 2013;21:1132–41.
34. Botter SM, van Osch GJ, Clockaerts S, Waarsing JH, Weinans H, van Leeuwen JP. Osteoarthritis induction leads to early and temporal subchondral plate porosity in the tibial plateau of mice: an in vivo microfocal computed tomography study. Arthritis Rheum 2011;63:2690–9.
35. Landells JW. The bone cysts of osteoarthritis. J Bone Joint Surg Br 1953;35:643–9.
36. Pallante-Kichura AL, Cory E, Bugbee WD, Sah RL. Bone cysts after osteochondral allograft repair of cartilage defects in goats suggest abnormal interaction between subchondral bone and overlying synovial joint tissues. Bone 2013;57:259–68.
37. Guzman RE, Evans MG, Bove S, Morenko B, Kilgore K. Mono-iodoacetate-induced histologic changes in subchondral bone and articular cartilage of rat femorotibial joints: an animal model of osteoarthritis. Toxicol Pathol 2003;31:619–24.
38. Shibakawa A, Yudoh K, Masuko-Hongo K, Kato T, Nishioka K, Nakamura H. The role of subchondral bone resorption pits in osteoarthritis: MMP production by cells derived from bone marrow. Osteoarthritis Cartilage 2005;13:679–87.
39. Tanamas SK, Wluka AE, Pelletier JP, Martel-Pelletier J, Abram F, Wang Y, *et al.* The association between subchondral bone cysts and tibial cartilage volume and risk of joint replacement in people with knee osteoarthritis: a longitudinal study. Arthritis Res Ther 2010;12:R58.
40. Kaspiris A, Khaldi L, Grivas TB, Vasiliadis E, Kouvaras I, Dagkas S, *et al.* Subchondral cyst development and MMP-1 expression during progression of osteoarthritis: an immunohistochemical study. Orthop Traumatol Surg Res 2013;99:523–9.
41. Wang M, Sampson ER, Jin H, Li J, Ke QH, Im HJ, *et al.* MMP13 is a critical target gene during the progression of osteoarthritis. Arthritis Res Ther 2013;15:R5.
42. Arokoski JP, Jurvelin JS, Vaatainen U, Helminen HJ. Normal and pathological adaptations of articular cartilage to joint loading. Scand J Med Sci Sports 2000;10:186–98.
43. Moskowitz RW, Davis W, Sammarco J, Martens M, Baker J, Mayor M, *et al.* Experimentally induced degenerative joint lesions following partial meniscectomy in the rabbit. Arthritis Rheum 1973;16:397–405.

Nagai et al. BMC Musculoskeletal Disorders 2014, 15:224
http://www.biomedcentral.com/1471-2474/15/224

BMC Musculoskeletal Disorders

RESEARCH ARTICLE Open Access

Contributions of biarticular myogenic components to the limitation of the range of motion after immobilization of rat knee joint

Momoko Nagai[1], Tomoki Aoyama[2], Akira Ito[1], Hirotaka Iijima[1], Shoki Yamaguchi[1], Junichi Tajino[1], Xiangkai Zhang[1], Haruhiko Akiyama[3] and Hiroshi Kuroki[1*]

Abstract

Background: Muscle atrophy caused by immobilization in the shortened position is characterized by a decrease in the size or cross-sectional area (CSA) of myofibers and decreased muscle length. Few studies have addressed the relationship between limitation of the range of motion (ROM) and the changes in CSA specifically in biarticular muscles after atrophy because of immobilization. We aimed to determine the contribution of 2 distinct muscle groups, the biarticular muscles of the post thigh (PT) and those of the post leg (PL), to the limitation of ROM as well as changes in the myofiber CSAs after joint immobilization surgery.

Methods: Male Wistar rats (n = 40) were randomly divided into experimental and control groups. In the experimental group, the left knee was surgically immobilized by external fixation for 1, 2, 4, 8, or 16 weeks (n = 5 each) and sham surgery was performed on the right knee. The rats in the control groups (n = 3 per time point) did not undergo surgery. After the indicated immobilization periods, myotomy of the PT or PL biarticular muscles was performed and the ROM was measured. The hamstrings and gastrocnemius muscles from the animals operated for 1 or 16 weeks were subjected to morphological analysis.

Results: In immobilized knees, the relative contribution of the PT biarticular myogenic components to the total restriction reached 80% throughout the first 4 weeks and decreased thereafter. The relative contribution of the PL biarticular myogenic components remained <20% throughout the immobilization period. The ratio of the myofiber CSA of the immobilized to that of the sham-operated knees was significantly lower at 16 weeks after surgery than at 1 week after surgery only in the hamstrings.

Conclusions: The relative contribution of the PT and PL components to myogenic contracture did not significantly change during the experimental period. However, the ratio of hamstrings CSAs to the sham side was larger than the ratio of medial gastrocnemius CSAs to the sham side after complete atrophy because of immobilization.

Keywords: Contracture, External fixators, Muscles, Range of motion, Rats

Background

The normal range of joint motion (ROM) is maintained by repeated daily movements. The normal ROM is difficult to restore once lost [1], and immobilization is a major cause of joint contracture. Physical therapy and surgical release are used to prevent and treat joint contracture [2-4]. Knee flexion contracture can be surgically treated by posterior soft tissue release such as hamstring lengthening, proximal gastrocnemius release, and posterior capsule release [2]. Studies on animal muscles have shown that passive extensibility depends on the size and length of the muscle fibers and the amount and arrangement of connective tissue in the muscle belly [5-7].

Contracture can occur when a muscle undergoes disuse, as in the case of limb immobilization [8]. The technique of fixation of muscles at abnormally short lengths can be used to study muscle atrophy [7,9,10]. In a

* Correspondence: kuroki.hiroshi.6s@kyoto-u.ac.jp
[1]Department of Motor Function Analysis, Human Health Sciences, Graduate School of Medicine, Kyoto University, 53 Shogoin, Kawahara-cho, Sakyo-ku, Kyoto 606-8507, Japan
Full list of author information is available at the end of the article

previous study, the components of joint contracture after immobilization were classified into arthrogenic and myogenic components [11]. However, to the best of our knowledge, no study has investigated the influence of myogenic components in detail. The low activity of immobilized muscles leads to muscle atrophy [9,12]. Muscle atrophy is caused by loss of tissue protein because of decreased synthesis and increased degradation [9,13], an increase in the amount of intramuscular connective tissue [14,15], and the arrangement of collagen fibrils in the endomysium [14,16,17]. Muscle atrophy from immobilization in shortened position is characterized by loss of muscle mass [18] and decrease in the size or cross-sectional area (CSA) of myofibers [19,20] and muscle length [5]. Few studies have addressed the relationship between muscle limitation of ROM and the changes in CSA specifically in biarticular muscles after atrophy because of immobilization.

The lower limb has three joints: the hip, knee, and ankle. The lower limb has many sites of muscle attachment. Biarticular muscles, in particular, are structurally coupled to the joints [21] and contribute strongly to myogenic restriction of ROM [22]. In the clinical situation, the hamstrings and gastrocnemius are often manipulated to prevent the progressive contracture or muscle atrophy when joint ROM is restricted [2,22-24]. The major focus of previous reports related to muscle CSAs and immobilization have been on monoarticular muscle [12,15,25]. However, the effect of joint immobilization on the myostatic properties and CSAs changes of biarticular muscles in the rat has not been extensively studied.

Our objective in this study was twofold: (1) to identify the relationship between biarticular muscles of the post thigh (PT; those muscles that cross the hip and knee joints) and those of the post leg (PL; those muscles that cross the knee and ankle joints) with the limitation of knee ROM after surgical immobilization and (2) to identify the relationship between the limitation of ROM at each phase of the contracture process and the changes in the CSA early (partial atrophy) and late (complete atrophy) after surgical immobilization.

Methods

Sample and surgical procedure

The experimental design for this study was approved by the College Animal Research Committee of Kyoto University (permission number: 12597). We used a total of forty 8-week-old male Wistar rats weighing 178–213 g randomly allocated in groups of 5 experimental and 3 control to the following five time points: 1, 2, 4, 8 and 16 weeks after surgical immobilization. The left hind limb of each experimental animal was immobilized with an external fixator consisting of wire and resin. Under sodium Nembutal anesthesia and sterile conditions, Kirschner wires were screwed into the femur and the tibia and fixed with wire and resin to maintain knee flexion of approximately 140° ± 5° (Figure 1). The flexed knee was thus rendered immobile. The right knee joint was subjected to sham surgery and was freely movable postoperatively. The control groups were included to control for the effect of age. The animals in each 1- and 16-weeks postsurgical experimental and control groups were used for morphological analysis. A high-resolution micro-CT scanner (SMX-100CT, Shimazu, Japan) was used to check the insertion site of the wires and view the immobilized leg. The leg was scanned from the ankle joint to the hip joint at the end of immobilization, i.e., when myotomy was performed. A bone and wire image was generated from the 3D image data sets by using a software (Amira 5.4, Visage, Germany).

All animals were housed in groups of 2 or 3 in plastic cages in an environmentally controlled room and fed rat food and water *ad libitum*.

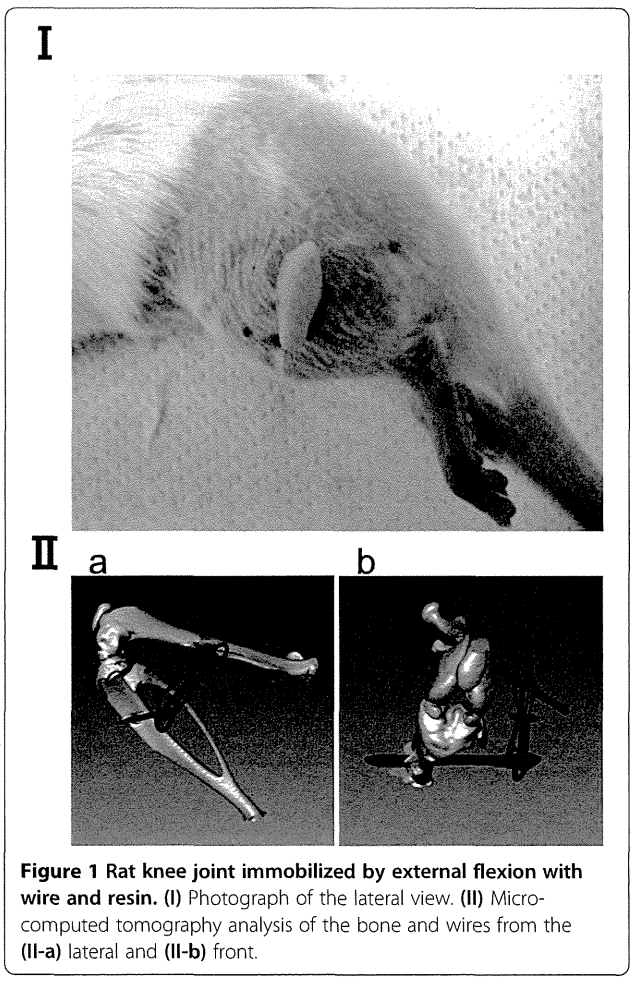

Figure 1 Rat knee joint immobilized by external flexion with wire and resin. (I) Photograph of the lateral view. **(II)** Micro-computed tomography analysis of the bone and wires from the **(II-a)** lateral and **(II-b)** front.

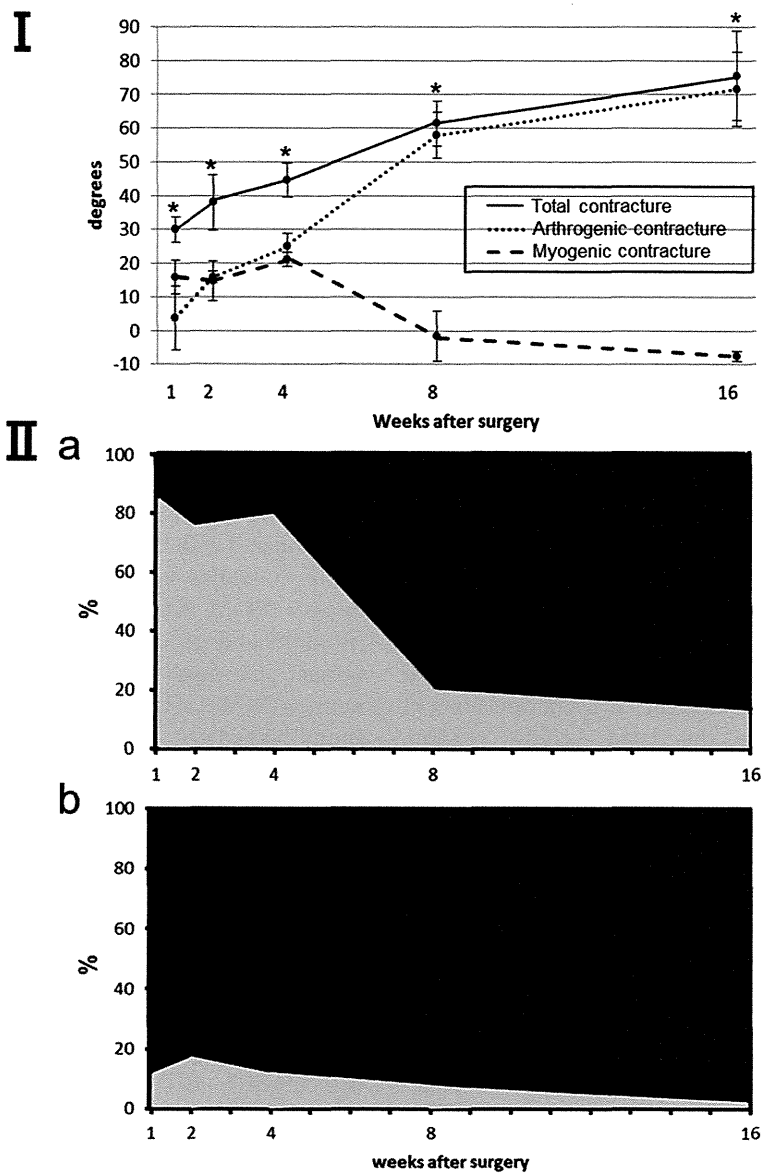

Figure 2 The myogenic and arthrogenic contractures in immobilized knee joints over time. (I) Results in degrees. As the duration of immobilization increased, the myogenic contracture decreased and the arthrogenic contracture increased. Values are presented as mean ± SD. *Significant difference in the restriction of extension ROM between the immobilized and sham knees. *$P < 0.05$. **(II)** Results as presented as the percent contributions of the biarticular muscles to the total restriction: **(II-a)** results for the PT, PT components shown in gray; results for other components shown in black; **(II-b)** results for the PL, PL components shown in gray; results for other components shown in black. The PT contribution peaked after the first week and decreased thereafter. The peak contribution of the PL was significantly less than that of the PT.

ROM analysis

At the end of the immobilization period, the animals were sacrificed under anesthesia with Nembutal and exsanguination. The wire and resin were removed from the joint and ROM analysis was performed. The macroscopic images were photographed with a digital camera (EX-V7, Casio, Japan) from the upper side. Thereafter the ROM was calculated using the Image J software package (National Institutes of Health, USA). The measurement method used was adopted from a previous study [25] and was slightly modified. We used a force gauge (DS2 series, Imada, Japan) to ensure that the direction and tension applied were the same as those in the original method. The ROM was defined as the angle (0° to 180°) between a straight line connecting the greater trochanter and the caput fibulae to a line connecting the caput fibulae and lateral malleolus with the hip joint at 90° of flexion. The maximum knee extension was defined as an extension of 180°. As the knee joint was extended passively for measurement, the trunk and

Table 1 Arthrogenic and myogenic contracture contributions to the total limitation of extension ROM

After immobilization	1 week	2 weeks	4 weeks	8 weeks	16 weeks
Total contracture	30.0 ± 4.1†	38.0 ± 9.0†	44.5 ± 5.5†	61.4 ± 7.5†	75.5 ± 14.8†
Myogenic contracture	15.9 ± 5.6	14.7 ± 6.5	21.0 ± 2.2	-1.6 ± 8.2‡	-7.5 ± 1.5‡
Arthrogenic contracture	3.7 ± 10.5	15.7 ± 1.9	25.0 ± 4.1	57.9 ± 7.6‡	71.5 ± 12.2‡

Values are given as mean ± SD. All data are presented in (°).
†Indicates significant difference was found when the given data were compared with sham data in the same time point.
‡Indicate significant difference was found when the given data were compared with the myogenic and arthrogenic contracture in the same time point.

pelvis were held manually to prevent the animal's body from sliding forward. As previously described [26], the probe of the force gauges used to measure the ROM was fitted to the distal part of the ankle and then the strings were pulled with a tension of 0.49 N in the direction perpendicular to the trunk to extend the knee joint. The maximum knee extension was measured three times: (1) when the limb was intact, (2) after removal of the skin and PT from the hind limb, and (3) after removal of the PL from the lower leg. The muscles were removed beginning with their distal attachments. Distal incisions of PT that broadly attached to the front of the tibia were made from the tibia to their origins (proximal attachments) at the ischial tuberosity. Distal incisions of the PL were made from the distal Achilles tendon, which adhered to the calcaneus, to their origins (proximal attachments) on the femur. The incisions were made with caution to avoid damage to any additional muscles.

Calculation of the arthrogenic and the PT and PL biarticular myogenic components of contracture

We evaluated myogenic contracture caused by the biarticular muscles of the leg, including their tendons and fascia, and arthrogenic contracture caused by the articular structures (bone, cartilage, synovium/subsynovium, capsule, and ligaments); myogenic and arthrogenic contractures were calculated with the use of the ROM measurements in the methods prescribed by Trudel et al [11]. The total contractures were independently calculated by the use of the ROM of experimental groups compared with those of sham-operated at each measurement time point to normalize. Myogenic contractures were further classified as those caused by PT or PL components. PT components were those crossing the hip and knee joints and PL components were those crossing the knee and ankle joints. The each of PT or PL components of myogenic contracture obtained after muscle detachment was used to estimate the each of biarticular muscles myogenic contracture. The each of PT or PL components of myogenic contracture were calculated by compared with the same sample.

The formulas used were as follows: (1) PT components = (ROM after biarticular myotomy at post thigh [immobilized group] – ROM before biarticular myotomy at post thigh [immobilized group]); (2) PL components = (ROM after biarticular myotomy at post limb [immobilized group] - ROM before biarticular myotomy at post limb [immobilized group]).

Morphological analysis

After myotomy of the biarticular muscles, we macroscopically confirmed the difference between the PT and PL. In the control group, the macroscopic images were photographed with a digital camera from the upper side. Serial cross sections of 10 μm were made using a cryostat (at -15°C); the portions from the middle part of the muscle belly of the bilateral hamstring and medial gastrocnemius muscles (CM1900, Leica, Germany) were stained with hematoxylin and eosin (H-E) for histological observation. Photographs (magnification: ×100) were taken of each section with a microscopy camera (ECLIPSE 80i, Nikon, Japan). A measuring field was defined over the entire muscle cross-section. The CSAs of at least 100 randomly selected muscle fibers were

Table 2 PT and PL of myogenic components in total extension ROM after knee joint immobilization

After immobilization	1 week	2 weeks	4 weeks	8 weeks	16 weeks
Total contracture (°)	30.0 ± 4.1	38.0 ± 9.0	44.5 ± 5.5	61.4 ± 7.5	75.5 ± 14.8
PT components (°) ratio of total (%)	25.6 ± 2.7	28.3 ± 7.5	35.1 ± 4.7	12.3 ± 5.2	10.0 ± 1.9
	82.4 ± 15.6	70.2 ± 20.0	66.5 ± 11.7	20.9 ± 10.6†	13.9 ± 4.6†
PL components (°) ratio of total (%)	3.9 ± 3.9	7.0 ± 5.3	5.6 ± 3.1	5.3 ± 3.9	2.1 ± 0.9
	12.5 ± 13.5	18.0 ± 14.8	12.7 ± 7.2	8.6 ± 6.8	2.7 ± 1.3

Values are given as mean ± SD.
†Indicates significant difference was found when the given data were compared with the data for 1, 2 and 4 weeks after surgery.

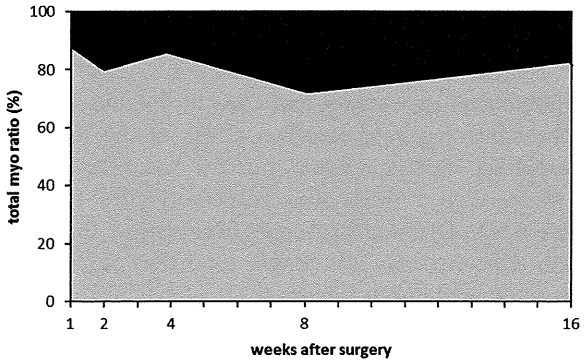

Figure 3 The percent contributions of the PT and PL to myogenic contracture. PL components shown in black; PT components shown in gray. The relative contributions of the PT and PL to myogenic contracture did not change throughout the experimental period.

measured using the Image J software program. Thereafter the mean fiber size of each muscle CSAs were calculated. Representative sections data are shown.

Statistical analysis

All data are shown as mean ± standard deviation (SD). The software program SPSS Statistics (IBM, USA) was used for statistical analysis. Differences in the ROM between the experimental and sham or control groups at each time point and differences in the CSAs of the hamstring and gastrocnemius muscles between the experimental periods were assessed using Student's *t*-test. The significant difference between the experimental and the sham or control groups at the same time point was measured at 95% CI not overlapping zero. One-way analysis of variance (ANOVA) and the Tukey-Kramer test were performed to examine differences in ROM among the time points.

Results

All of the rats survived, gained weight, and remained active throughout the experimental period. Neither prolonged edema nor acute inflammation was observed in any animal.

ROM analysis and relationship between the myogenic and arthrogenic components of contracture

The loss of extensional ROM was fairly similar between sham-operated and control knees except at the 4-week time point. Four week after surgery, the extensional ROM in the sham knees was smaller than that in the control animals ($P = 0.04$, data not shown). Knee extension was significantly restricted in all experimentally immobilized knee

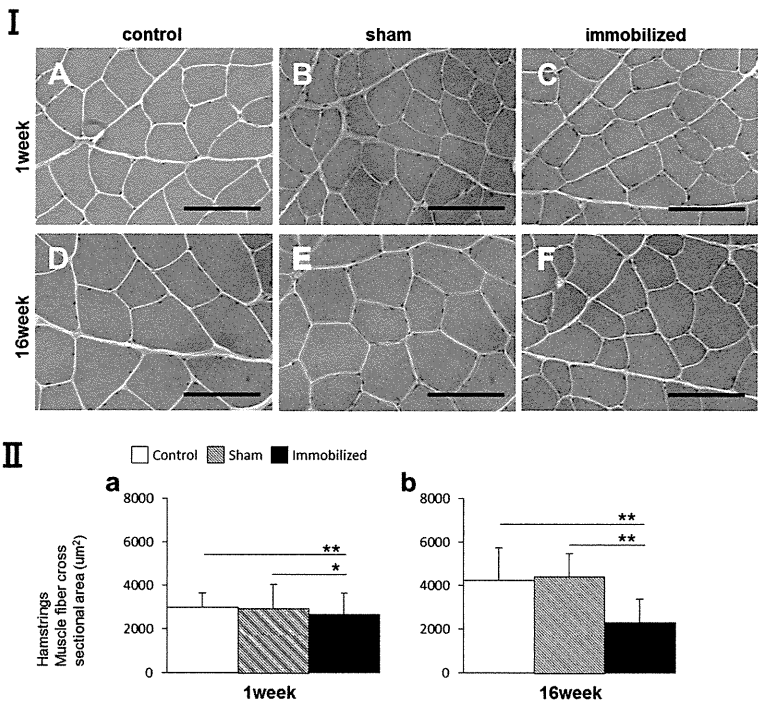

Figure 4 Morphological analysis and myofiber CSAs measurements (μm^2) of the hamstring muscle. (I) The CSA of the hamstring muscles of control, sham-operated, and immobilized knees after 1 and 16 weeks. **(A, D)** Control group. **(B, E)** Sham-operated knees. **(C, F)** Immobilized knees. Scale bars represent 100 μm (microscope magnification: ×400). **(II-a, b)** Measurement of the CSA (μm^2) of the hamstring muscles (only one displayed). Values are presented as mean ± SD; $^{*}P < 0.05$; $^{**}P < 0.001$. The CSA in the immobilized knees was lower than that in the control or sham knees at both time points.

joints as compared with that in sham-operated knee joints, at the same time point ($P < 0.05$; Figure 2 I; Table 1). The myogenic contracture peaked 4 weeks after surgery and decreased thereafter. The arthrogenic contracture progressed especially rapidly between postoperative weeks 4 and 8. The myogenic contracture in the immobilized knees was significantly lower than the arthrogenic contracture at the 8- and 16-week time points ($P < 0.01$; Table 1).

PT and PL components involved in the limitation of extension angular displacement

In the immobilized knees, the relative contribution of the PT components to the total restriction reached 82.4 ± 15.6% after the first postoperative week but decreased thereafter and was significantly low 8 and 16 weeks after surgery ($P < 0.01$; Figure 2 II-a, Table 2). The relative contribution of the PL components reached 18 ± 14.8% after 2 weeks and throughout the remainder of the immobilization period (Figure 2 II-b, Table 2). However, the ratio of the PT and PL contributions to the myogenic contracture did not change throughout the experimental period ($R^2 = 0.006$; Figure 3). In the sham-operated knees, the relative contribution of the PT components to the myogenic contracture was >76% and almost plateaued throughout the experimental period similar to the immobilized knees.

Morphological appearance and CSAs of the muscle fibers

In the control group, myofiber CSAs of the hamstring and medial gastrocnemius muscles were larger after 16 weeks than 1 week after surgery (Figure 4 I-A, D; Figure 5 I-A, D). In macroscopic observation, the muscle length of hamstrings was longer than that of gastrocnemius in control group (Figure 6).

The CSAs of hamstring muscle fiber

After 1 and 16 postoperative weeks, the CSAs of the hamstring of the immobilized knees were found to be significantly smaller than those of the sham-operated or the control group ($^{*}P < 0.05$; Figure 4 II-a, $^{**}P < 0.001$; Figure 4 II-a,b). These trends were similar to all samples.

The CSAs of medial gastrocnemius muscle fiber

After 1 and 16 postoperative weeks, the CSAs of the medial gastrocnemius muscles of the immobilized knees were significantly smaller than those of the sham-operated or control group. One week after surgery, the

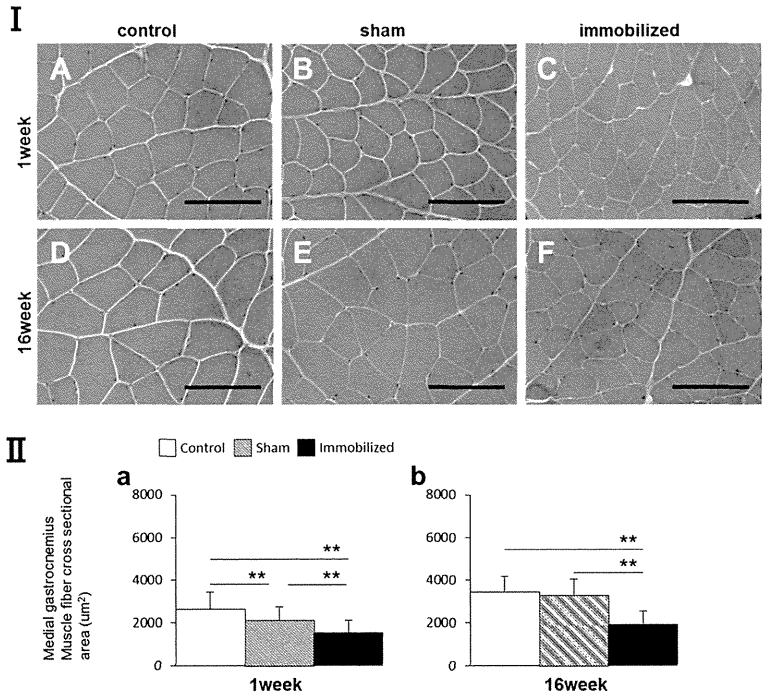

Figure 5 Morphological analysis and myofiber CSA measurements (μm²) of the medial gastrocnemius muscle. (I) The CSAs of the medial gastrocnemius muscle from the control, sham-operated, and immobilized knees after 1 and 16 weeks. **(A, D)** Control group. **(B, E)** Sham-operated knees. **(C, F)** Immobilized knees. Scale bars represent 100 μm (microscope magnification: ×400). **(II-a, b)** Measurement of the CSA (μm²) of the medial gastrocnemius muscle (only one displayed). Values are presented as mean ± SD; $^{**}P < 0.001$. The CSA in the immobilized knees was lower than that of the control or sham knees at both time points.

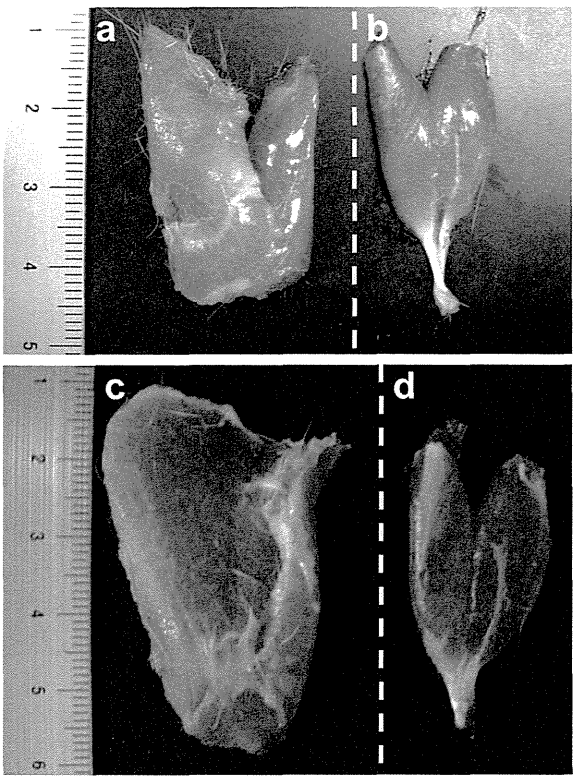

Figure 6 Macroscopic observation of PT and PL of the control group after 1 and 16 weeks. (a) PT at the 1-week, **(b)** PL at 1 week, **(c)** PT at 16 weeks, **(d)** PL at 16 weeks. The dotted line shows the medial side. The muscle length of PT (including the hamstrings) were longer than that of PL (including the gastrocnemius).

CSAs of the medial gastrocnemius muscles of the sham-operated knees were significantly smaller than those of the control group ($^{**}P < 0.001$; Figure 5 II-a,b). These trends were similar to all samples.

Comparison of the hamstring and gastrocnemius CSAs

In histologically, the myofiber CSAs of the hamstring were larger than those of the gastrocnemius muscles at each time point in the sham and immobilized knees (Figures 4, 5 I). The CSAs of the hamstring were significantly larger than those of the medial gastrocnemius muscles at each time point in the all groups ($P < 0.01$; Figure 7-a,b,c), except for at 1 week in the control group (Figure 7-a). The CSAs of each muscles at 16 weeks were significantly larger than those at 1 week in the all groups ($P < 0.01$), except for those of the gastrocnemius in the control group ($P < 0.05$). The ratio of the hamstring CSAs of the immobilized knee to those of the sham-operated knee significantly decreased between postoperative weeks 1 and 16 ($P < 0.05$; Figure 7-d); however, the ratio for the gastrocnemius did not significantly change.

Discussion

In the present study, the myogenic contracture in the immobilized knee have significantly deceased than arthrogenic contracture after 8 week time point. However, the relative contribution of the PT and PL components to the myogenic contracture did not significantly change throughout the experimental period. This results suggested that the PT components had a greater impact than the PL components on the muscle contracture through the experimental period. Immobilization in a shortened position produced the most extreme muscle atrophy due to significant shortening of the fibers and reduction in the CSA [18-20]. It suggested that both of PT and PL muscles have got atrophy and they lead muscle ROM limitation.

In the immobilized knees, the relative contributions of the PT and PL to the total contracture and the myogenic contracture exhibited different tendencies between the early and late of experimental period. The ratio of the CSAs of the hamstring of the immobilized knees to those of the sham side was significantly smaller after 16 weeks than after 1 week of immobilization. However, the CSAs of the gastrocnemius did not change remarkably at both of the early and late time point. In the present study, immature rats were treated. Muscle fiber diameter increases dramatically during early growth animals. The peak change in the increased diameter and fiber number differs for each of muscle [14]. Owing to aging, the compensatory hypertrophy of some fibers brought about by the normal increase in body weight resulted in increased load on the muscle [27]. The pathways that contribute to the increase in apoptosis observed in acutely atrophying muscle differ strikingly according to the age [28] and muscle type [4,14,20].

In this study, the myofiber CSAs were larger in the hamstrings than in the gastrocnemius muscle in all groups. We confirmed that the muscle length of hamstrings was longer than that of gastrocnemius in the control group. The muscle mass was calculated by multiplying the CSA and the muscle length [29]. A previous study on the muscle architecture of the rat hind limb, showed that the muscle fiber length of the hamstrings was larger than that of the gastrocnemius [30]; this holds true for humans too [31]. Muscle mass can influence the self-inertia of a joint [32]. Passive extensibility is influenced by the size (mass) and length of muscle fibers [5,33] and the amount and arrangement of the connective tissues of the muscle belly [5]. This means that the muscle length and CSAs of the PT (including the hamstrings) were larger than those of the PL (including the gastrocnemius), suggesting that PT was more effective than PL in restricting the muscle extensibility because of increased collagen fibers in its connective tissues.

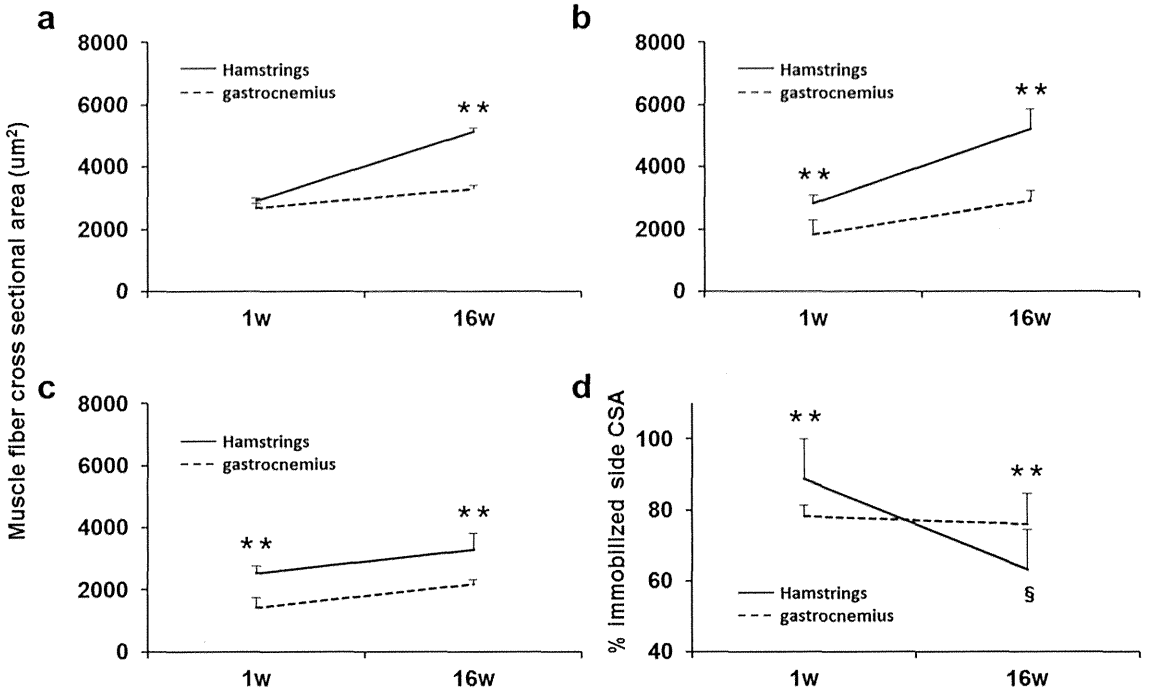

Figure 7 Changes in the CSAs and comparison of hamstring and gastrocnemius cross sectional areas during the experimental periods. Cross-sectional area (μm^2) of the control group **(a)**, sham-operated group **(b)**, and immobilized group **(c)**. The ratio of the immobilized side CSA to the sham side CSA (%) **(d)**. Values are presented as mean + SD; **, hamstring vs gastrocnemius at the same time point ($P < 0.01$); §, 1 week vs 16 weeks of hamstring ($P < 0.01$). Significant differences were found the CSAs between the hamstring and the medial gastrocnemius muscles at each time point in the all groups, except for at 1 week in the control group. The ratio was significantly lower after 16 weeks than after 1 week for the hamstring but not for the gastrocnemius. The myofiber CSAs of the hamstring were larger than those of the gastrocnemius at each time point in all groups, except for at 1 week in control group.

In addition, one potential explanation is that the difference in the contributions of the PT and PL could also be attributed to the difference in their lever arms, i.e., the distance between the point at which a force is applied and the axis. Notably, the lever arm of a muscle depends on the distance between its attachment points. According to one study on the muscles of the frog legs, the relationship between the moment arm and sarcomere length related to each proximal and distal joint angle [6]. However the length of the moment arm of the biarticular muscle is not always equal to the one located distal or proximal to it [34]. The PL components in this study originated very close to the axes of rotation of the knee and ankle, their effective lever arms very small. However, the PT distally and broadly extended on the front of the tibia, so their lever arms were larger than those of the PL, a result suggesting that the PT lengthens more than the PL during extension. Passive stretch and isometric tension are suggested to stimulate protein synthesis [9] and thus increase extensibility [22,32]. In this study, the PT components contributed more than the PL components to myogenic contracture, suggesting that knee joint immobilization restricted the extension of the PT more than it did of the PL, thereby promoting pronounced PT atrophy.

This relationship and other changes in the biarticular muscles of the legs after immobilization are worthwhile topics for future research.

Limitations

In this study, we measured the ROM of the knee joint adjacent to a freely mobile ankle joint. The traction string was attached to the calcaneus, but the influence of the ankle joint may not have been fully evaluated. Passive plantar flexion of the talocrural joint would have allowed us to better evaluate the collective contribution of the PL to the myogenic contracture. There were technical limitations associated with the arthrometer. For quantitative evaluation, we used a force gauge with the moment arm manually held, but manually applied power generates an inaccurate torque. Nevertheless, the loss of angle and the gradual increase in arthrogenic contracture after 4, 8, and 16 weeks in our study were similar to those mentioned in a previous report [11], suggesting that our method was reasonably accurate. With regard to study design, it is advisable to use a large sample size and to choose sample by randomly detaching each biarticular muscle.

Conclusions

This report showed that the relative contribution of the PT and PL components to myogenic contracture did not significantly change during the experimental period. However, the ratio of hamstring CSAs to the sham side was larger than the ratio of medial gastrocnemius CSAs to the sham side after complete atrophy because of immobilization. In conclusion, our findings suggest that the contribution of the biarticular muscles to the limitation in the knee extension ROM after knee joint immobilization was predominantly caused by PT rather than PL.

Abbreviations

PT: Biarticular muscles at the post thigh, which means behind the thigh; PL: Biarticular muscles at the post leg, which means behind the leg; ROM: Range of joint motion; CSA: Cross-sectional area.

Competing interests

The authors declare that they have no competing interests.

Authors' contributions

MN, TA, AI, HI, SY, JT, XZ, HA, HK carried out conception or design of the study and were involved in the analysis and interpretation of the data. MN, TA, AI, HI, SY, JT, HK were involved in preparing the draft and conducting the statistical analysis. MN, TA, and HK approved the final version to be published. HK is the laboratory chair and obtained the funding. MN carried out the collection and assembly of data. All authors read and approved the final manuscript.

Acknowledgments

The authors thank Tetsuya Takakuwa, Rune Fujioka, and Ryota Takaishi (Kyoto University, Kyoto) for their technical assistance. The authors thank Naoto Fujita (Hiroshima University, Hiroshima) for his knowledgeable advice. This study was supported in part by the Grants-in-Aid for Scientific Research in Japan #20240057.

Author details

[1]Department of Motor Function Analysis, Human Health Sciences, Graduate School of Medicine, Kyoto University, 53 Shogoin, Kawahara-cho, Sakyo-ku, Kyoto 606-8507, Japan. [2]Department of Development and Rehabilitation of Motor Function, Human Health Sciences, Graduate School of Medicine, Kyoto University, Kyoto, Japan. [3]Department of Orthopaedic Surgery, Graduate School of Medicine, Gifu University, Gifu, Japan.

Received: 30 October 2013 Accepted: 1 July 2014
Published: 7 July 2014

References

1. Hildebrand KA, Sutherland C, Zhang M: **Rabbit knee model of post-traumatic joint contractures: the long-term natural history of motion loss and myofibroblasts.** *J Orthop Res* 2004, **31**:313–320.
2. van Bosse HJ, Feldman DS, Anavian J, Sala DA: **Treatment of knee flexion contractures in patients with arthrogryposis.** *J Pediatr Orthop* 2007, **27**:930–937.
3. Frank C, Akeson WH, Woo SL, Amiel D, Coutts RD: **Physiology and therapeutic value of passive joint motion.** *Clin Orthop Relat Res* 1984, **185**:113–125.
4. Oates BR, Glover EI, West DW, Fry JL, Tarnopolsky MA, Phillips SM: **Low-volume resistance exercise attenuates the decline in strength and muscle mass associated with immobilization.** *Muscle Nerve* 2010, **42**:539–546.
5. Gajdok RL: **Passive extensibility of skeletal muscle: review of the literature with clinical implications.** *Clin Biomech* 2001, **16**:87–101.
6. Mai MT, Lieber RL: **A model of semitendinosus muscle sarcomere length, knee and hip joint interaction in the frog hind limb.** *J Biomech* 1990, **23**:271–279.
7. Booth FW, Seider MJ: **Early change in skeletal muscle protein synthesis after limb immobilization of rats.** *J Appl Physiol* 1979, **47**:974–977.
8. Nesterenko S, Morrey ME, Abdel MP, An KN, Steinmann SP, Morrey BF, Sanchez-Sotelo J: **New rabbit knee model of posttraumatic joint contracture: indirect capsular damage induces a severe contracture.** *J Orthop Res* 2009, **27**:1028–1032.
9. Goldspink DF: **The influence of immobilization and stretch on protein turnover of rat skeletal muscle.** *J Physiol* 1977, **264**:267–282.
10. Ishikawa T, Shimizu M, Mikawa Y, Zhu BL, Quan L, Li DR, Zhao D, Maeda H: **Pathology of experimental disuse muscular atrophy in rats.** *Connect Tissue Res* 2005, **46**:101–106.
11. Trudel G, Uhthoff HK: **Contractures secondary to immobility: is the restriction articular or muscular? An experimental longitudinal study in the rat knee.** *Arch Phys Med Rehabil* 2000, **81**:6–13.
12. Booth FW: **Effect of limb immobilization on skeletal muscle.** *J Appl Physiol* 1982, **52**:1113–1118.
13. Spector SA, Simard CP, Fournier M, Sternlicht E, Edgerton VR: **Architectural alterations of rat hind-limb skeletal muscles immobilized at different lengths.** *Exp Neurol* 1982, **76**:94–110.
14. Järvinen TA, Józsa L, Kannus P, Järvinen TL, Järvinen M: **Organization and distribution of intramuscular connective tissue in normal and immobilized skeletal muscles. An immunohistochemical, polarization and scanning electron microscopic study.** *J Muscle Res Cell Motil* 2002, **23**:245–254.
15. Borg TK, Caulfield JB: **Morphology of connective tissue in skeletal muscle.** *Tissue Cell* 1980, **12**:197–207.
16. Okita M, Yoshimura T, Nakano J, Motomura M, Eguchi K: **Effects of reduced joint mobility on sarcomere length, collagen fibril arrangement in the endomysium, and hyaluronan in rat soleus muscle.** *J Muscle Res Cell Motil* 2004, **25**:159–166.
17. Alnaqeeb MA, Goldspink G: **Changes in fibre type, number and diameter in developing and ageing skeletal muscle.** *J Anat* 1987, **153**:31–45.
18. Dupont-Versteegden EE: **Apoptosis in skeletal muscle and its relevance to atrophy.** *World J Gastroenterol* 2006, **12**:7463–7466.
19. Boonyarom O, Inui K: **Atrophy and hypertrophy of skeletal muscles: structural and functional aspects.** *Acta Physiol* 2006, **188**:77–89.
20. Zhang P, Chen X, Fan M: **Signaling mechanisms involved in disuse muscle atrophy.** *Med Hypotheses* 2007, **69**:310–321.
21. Zajac FE: **Understanding muscle coordination of the human leg with dynamical simulations.** *J Biomech* 2002, **35**:1011–1018.
22. Rushton A, Spencer S: **The effect of soft tissue mobilisation techniques on flexibility and passive resistance in the hamstring muscle-tendon unit: a pilot investigation.** *Man Ther* 2011, **16**:161–166.
23. Kwah LK, Herbert RD, Harvey LA, Diong J, Clarke JL, Martin JH, Clarke EC, Hoang PD, Bilston LE, Gandevia SC: **Passive mechanical properties of gastrocnemius muscles of people with ankle contracture after stroke.** *Arch Phys Med Rehabil* 2012, **93**:1185–1190.
24. Whatman C, Knappstein A, Hume P: **Acute changes in passive stiffness and range of motion post-stretching.** *Phys Ther Sport* 2006, **7**:195–200.
25. Usuba M, Miyanaga Y, Miyakawa S, Maeshima T, Shirasaki Y: **Effect of heat in increasing the range of knee motion after the development of a joint contracture: an experiment with an animal model.** *Arch Phys Med Rehabil* 2006, **87**:247–253.
26. Fukui N, Tashiro T, Hiraoka H, Oda H, Nakamura K: **Adhesion formation can be reduced by the suppression of transforming growth factor-beta1 activity.** *J Orthop Res* 2000, **18**:212–219.
27. Rowe RW, Goldspink G: **Muscle fibre growth in five different muscles in both sexes of mice.** *II Dystrophic Mice J Anat* 1969, **104**:531–538.
28. Williams PE, Goldspink G: **Longitudinal growth of striated muscle fibres.** *J Cell Sci* 1971, **9**:751–767.
29. Lieber RL, Blevins FT: **Skeletal muscle architecture of the rabbit hind limb: functional implications of muscle design.** *J Morphol* 1989, **199**:93–101.
30. Eng CM, Smallwood LH, Rainiero MP, Lahey M, Ward SR, Lieber RL: **Scaling of muscle architecture and fiber types in the rat hind limb.** *J Exp Biol* 2008, **211**:2336–2345.
31. Grosset JF, Onambele-Pearson G: **Effect of foot and ankle immobilization on leg and thigh muscles' volume and morphology: a cases study using magnetic resonance imaging.** *Anat Rec* 2008, **291**:1673–1683.
32. Samukawa M, Hattori M, Sugama N, Takeda N: **The effects of dynamic stretching on plantar flexor muscle-tendon tissue properties.** *Man Ther* 2011, **16**:618–622.